27742

National Library of Canada | Bibliothèque nationale du Canada

CANADIAN THESES ON MICROFICHE | THÈSES CANADIENNES SUR MICROFICHE

NAME OF AUTHOR *NOM DE L'AUTEUR* Michael Ray Sinclair

TITLE OF THESIS *TITRE DE LA THÈSE* Aspects of Rural and Metropolitan Unemployment in Selected Countries

UNIVERSITY *UNIVERSITÉ* University of Guelph

DEGREE FOR WHICH THESIS WAS PRESENTED *GRADE POUR LEQUEL CETTE THÈSE FUT PRÉSENTÉE* Master of Science

YEAR THIS DEGREE CONFERRED *ANNÉE D'OBTENTION DE CE GRADE* 1975

NAME OF SUPERVISOR *NOM DU DIRECTEUR DE THÈSE* Dr. Orville Grey

Permission is hereby granted to the NATIONAL LIBRARY OF CANADA to microfilm this thesis and to lend or sell copies of the film.

The author reserves other publication rights, and neither the thesis nor extensive extracts from it may be printed or otherwise reproduced without the author's written permission.

L'autorisation est par la présente, accordée à la BIBLIOTHÈQUE NATIONALE DU CANADA de microfilmer cette thèse et de prêter ou de vendre des exemplaires du film.

L'auteur se réserve les autres droits de publication; ni la thèse ni de longs extraits de celle-ci ne doivent être imprimés ou autrement reproduits sans l'autorisation écrite de l'auteur.

DATED *DATÉ* [illegible] SIGNED *SIGNÉ* [signature]

PERMANENT ADDRESS *RÉSIDENCE FIXE* #27-22 Morrow Ave

Winnipeg, Manitoba

R2M 1H1

NL-91 (3-74)

THE UNIVERSITY OF ALBERTA

ASPECTS OF OVULE AND MEGAGAMETOPHYTE DEVELOPMENT IN *EPHEDRA NEVADENSIS*

by

MICHAEL JOHN SUMNER

A THESIS

SUBMITTED TO THE FACULTY OF GRADUATE STUDIES AND RESEARCH IN PARTIAL FULFILLMENT OF THE REQUIREMENTS FOR THE DEGREE OF

MASTER OF SCIENCE

IN

PLANT ANATOMY

DEPARTMENT OF BOTANY

EDMONTON, ALBERTA

SPRING, 1976

THE UNIVERSITY OF ALBERTA

FACULTY OF GRADUATE STUDIES AND RESEARCH

The undersigned certify that they have read, and recommend to the Faculty of Graduate Studies and Research, for acceptance, a thesis entitled "Aspects of Ovule and Megagametophyte Development in Ephedra nevadensis."

submitted by: Michael John Sumner

in partial fulfillment of the requirements for the degree of Master of Science in Plant Anatomy.

David W. Ewis
Supervisor

Date: September 3, 1975.

ABSTRACT

A study of ovule ontogeny in Ephedra nevadensis was made using improved microtechnical methods for light microscopy. The stages of ovule development from megasporogenesis to fertilization are reconsidered in the context of total ovule expansion.

Two ovules are borne in the axils of the uppermost pair of decussate ovulate cone bracts. The ovule consists of a megagametophyte surrounded by an extensive nucellus, enclosed by two asymmetric integuments. A single sporogenous cell is differentiated in the hypodermis of the nucellus. The sporogenous cell divides into a micropylar parietal cell and a chalazal megaspore mother cell. A crassinucellate ovule is produced by periclinal divisions of the parietal cell, hypodermal nucellar cells, and the nucellar epidermis. The megagametophyte exhibits monosporic development. The megaspore mother cell divides meiotically to produce a chalazal functional megaspore surmounted by three degenerate megaspores. Homeotypic meiosis is staggered; the chalazal dyad cell undergoes a second meiotic division prior to the micropylar dyad cell. The functional megaspore nucleus undergoes an extended period of nuclear divisions to produce a large, coenocytic gametophyte. The coenocytic megagametophyte becomes cellular by the centripetal growth of tubular alveoli. Two archegonia are differentiated at the micropylar end of megagametophyte. Each archegonium is made up of a bilayer of

jacket cells enclosing a large central cell. Micrographic evidence for the process of syngamy is presented for the first time in the genus. Growth of the nucellus as correlated with gametophyte development is discussed.

ACKNOWLEDGMENT

The constructive criticism and review of the manuscript by my supervisor, Dr. David Cass, are gratefully acknowledged. Much appreciation to Dr. Wilson Stewart and Dr. Dale Vitt for the help and suggestions they gave me during the preparation of this thesis. I am indebted to the able skills and willingness of Ilana Karas for her help with the techniques of light microscopy. I am deeply indebted to my wife, Marie, for her assistance in the field and in the laboratory and for her patience over the duration of this thesis. Research for this thesis has been supported by National Research Council Grant A6103 to David D. Cass.

TABLE OF CONTENTS

LIST OF FIGURES

CHAPTER ONE

GENERAL INTRODUCTION AND LITERATURE REVIEW

The gymnospermous taxon Gnetopsida is represented by three genera of extant plants: Ephedra, Gnetum, and Welwitschia. Ephedra is the sole representative of the group in North America. In 1889, Stapf subdivided the thirty-two known species of Ephedra into three sections: Alatae, Asarca, and Pseudobaccatae based on the morphology of the mature megasporangiate cone bracts (Pearson 1929). The precise number of species of Ephedra is debatable. Foster and Gifford (1974) list 35 species; Andrews (1961) lists 42. The genus is widely distributed along two world belts. One belt, comprising the northern hemisphere species, runs approximately between 30 degrees N latitude and 42 degrees N latitude. It includes the southwestern United States, the Mediterranean region of Europe, and Western and Central Asia. The second belt runs southward through South America from Equador to Chile and eastward into parts of Brazil and Argentina (Pearson 1929). The 16 North American species are confined to the cold desert regions of California, Nevada, Oregon, Utah, Arizona, and New Mexico. No species of Ephedra is found east of the Rocky Mountains except Ephedra antisyphilitica which extends into the Texas prairies (Cutler 1939).

Vegetative Morphology

The vegetative morphology of Ephedra is remarkably uniform, most species being profusely branched shrubs characterized by distinct nodes and internodes. The shoot apical meristem exhibits a tunica-corpus mode of organization similar to that found in Gnetum, Welwitschia and in the angiosperms (Gifford 1943). The ensheathing leaves are small with a much reduced lamina and are arranged in alternating whorls of two or three at the node (Foster 1972). The leaves are deciduous during later stages of shoot ontogeny. The stem is modified to perform the assimilatory function of the plant. The internodal region of the stem is composed of longitudinal ridges and furrows. The stomata, which exhibit a haplocheilic mode of development (Pant and Mehra 1964) occur in furrows of the stem. The cortical tissue immediately subepidermal to the stomata is organized into loose chlorenchyma. A thick cutical covers the epidermis of the stem. The vascular system of the internodal region of the stem is composed of six to seventeen collateral bundles exhibiting endarch maturation of primary xylem (Marsden and Steeves 1955). The tracheids of the primary and secondary xylem are gymnospermous in nature with circular bordered pits occurring on the radial and tangential walls (Thompson 1912). The secondary xylem is initiated from a continuous vascular cambium and is made up in part of vessel members exhibiting a unique type of perforation plate, termed foraminate (Esau 1965).

Reproductive Morphology

Ephedra is dioecious, though rare monoecious plants have been described (Land 1907, Mehra 1950). The microsporangiate cone consists of a short axillary shoot bearing from two to eight pairs of opposite and decussate bracts (Land 1904). The lowermost pair of bracts are sterile. A short microsporangiate shoot is borne in the axil of each of the remaining bracts. The microsporangiate shoot is made up of an axis bearing a pair of basally fused bracteoles which enclose a terminal group of 5 to 6 microsporangia (Eames 1952). The microspores derived by meiosis are shed from the loculus of the microsporangium in the four-nucleate stage: two sperm cells, a stalk cell, and a tube nucleus (Land 1904). The two prothallial cells degenerate prior to dehiscence. Bold (1967) is of the opinion that the generative cell in Ephedra antisyphilitica forms the two sperm nuclei directly, rather than first dividing into a body and stalk cell as in the other described species of Ephedra (Martens 1971). Typically two ovules are borne in axils of the distal cone bracts, though uniovulate species have been described (Land 1907). The process of megasporogenesis and megagametogenesis is as described in this thesis. Following fertilization there is a period of free-nuclear zygotic division to produce eight diploid nuclei in the central cell cytoplasm. Each becomes cellular and has the potential to become an embryo (Chamberlain 1935). In Ephedra the proembryo cell in chalazal region of the central cell usually develops into the dicotyledonous embryo.

History and Taxonomy

The genus Ephedra was first described by Tournefort in 1703 (Arber and Parkin 1908). Linnaeus accepted Tournefort's genus Ephedra and placed it in the fifteenth group, the coniferae, following the genus Taxus. In 1827 Robert Brown published a paper "on the Structure of the Female Flower in Cycadeae and Coniferae" in which he described the naked megasporangium of the cycads and conifers, in contrast to the enclosed ovules of angiosperms. Brown extended the lack of an investing carpel to include Ephedra and the genus Gnetum, originally described by Rumphius (Arber and Parkin 1908). Brongniart in 1843, utilizing the important observations of Brown, was the first systematist to raise the gymnosperms to a rank equivalent to that of the dicotyledons with Ephedra and Gnetum occupying a subordinate position within the group. In 1867 Parlatore divided the Gymnospermae into three groups of equivalent rank: Gnetaceae, Coniferae, and Cycadaceae. The Gnetaceae included by this time a third genus Welwitschia. The presence of vessels in the secondary xylem, the compound nature of both the male and female strobili, and the long micropylar tube formed by the innermost envelope united Ephedra, Gnetum, and Welwitschia into a single group and provided evidence for their separation from the rest of the Gymnospermae (Chamberlain 1935). Many of the early morphologists saw in the Gnetaceae a combination of reproductive and vegetative characters, in particular the presence of vessels in the secondary xylem, which suggested

a connecting link between the angiosperms and the Gnetales (Thompson 1912). Later, in 1918, Thompson showed that the vessels in the angiosperms and the Gnetales, though somewhat similar in mature morphology, were of different ontogenetic origin. Subsequent publication on the Gnetales began to emphasize the heterogeneous nature of the group. Eames (1952) provided morphological evidence to support a division of the old order Gnetales and the establishment of three orders, Ephedrales, Gnetales (sensu stricto) and Welwitschiales, each to contain one family. Eames based his argument on a study of the megasporangiate and microsporangiate cones of Ephedra in which he contended that the ovule of Ephedra is appendicular and not cauline as is the case in Gnetum and Welwitschia.

The lack of megafossil evidence (Andrews 1963) makes an elucidation of the true phylogeny of Ephedra difficult. The answer must therefore be found in the area of extant plant morphology. The present study was undertaken to examine the ovule morphology of Ephedra nevadensis with the hope of confirming old and providing new information on the reproductive biology of Ephedra by using improved histological techniques.

CHAPTER TWO

OVULE AND MEGAGAMETOPHYTE ONTOGENY

INTRODUCTION

Details of ovule ontogeny in Ephedra were first described by Strasburger (1879) in which he described the stages of late megagametogenesis and early embryo development in Ephedra altissima. Land (1904, 1907) published a relatively complete description of megagametogenesis and embryogenesis in Ephedra trifurca, but the line diagrams illustrated the isolated gametophyte without considering the nucellar and integumentary tissues. Numerous short publications on the reproductive biology of Ephedra have appeared in the literature since the two articles by Land. These have been summarized by Pearson (1929) and Martens (1971).

There is general agreement among all the authors that development of the megagametophyte in Ephedra follows a typical gymnospermous pattern. The megagametophyte is monosporic in origin and goes through an extended period of free nuclear divisions followed by the formation of cell walls. Depending on the species, two to nine archegonia are formed at the micropylar end of the megagametophyte.

The present study re-examines the process of megagametogenesis in Ephedra and provides for the first time, a detailed account of megasporogenesis in the genus. An attempt has been made to correlate the development of the megagametophyte

with the corresponding periods of integument and nucellar ontogeny. By using micrographs in conjunction with improved microtechnique, it is hoped that a better understanding of the ovule as a developmental system can be generated.

MATERIALS AND METHODS

Collection

In order to obtain a complete series of developmental stages, ovulate cones of Ephedra nevadensis Wats. were collected from two locations differing in elevation and latitude. Ovulate cones illustrating megasporogenesis and the early stages of gametophytic free nuclear division were collected from an area west of Reno, Nevada (39 degrees N latitude and 119 degrees W longitude), between May 6, 1974 and May 8, 1974. Ovulate cones illustrating both the early and later stages of megagametongenesis were collected from an area south of Bishop, California (37 degrees N latitude and 118 degrees W longitude) between April 24, 1974 and May 5, 1974. Reference plants of Ephedra nevadensis were transplanted into plastic pots and are presently housed at the Department of Botany greenhouse, University of Alberta, Edmonton, Alberta. All ovulate cones were collected in the early morning and transported back to campsite in moist paper towels. Fixation was initiated by the afternoon of the same day.

Microtechnique

Two methods of chemical fixation were employed; one utilizing F.A.A. in 50% ethanol (Johansen 1940), the other utilizing 3% phosphate-buffered (pH 6.8) glutaraldehyde

(Ladd Research Industries, Inc., Burlington, Vermont). For the material to be fixed in F.A.A., whole ovulate cones were placed in 100 ml. vials containing the fixative for period of four weeks, then transferred to 50% ethanol for storage. The outer integument becomes sclerified during ovule ontogeny and to facilitate the complete exchange between embedding medium and solvent, this outer envelope was frequently dissected away. The tissue for paraffin microtomy was passed through an ethanol-tertiary butyl alcohol series (Johansen 1940) and embedded in "Paraplast Plus" (M.P. 56 degrees C - 57 degrees C). Paraffin blocks were sectioned at 10 um on a Spencer Model AO rotary microtome and the paraffin ribbons were affixed to glass slides with Haupt's adhesive (Jensen 1962). The paraffin was removed from the sections by passing them through a xylene-alcohol series (Jensen 1962). The sections were stained in aqueous safranin-fast green or alternatively with 0.05% Toluidine blue O in 0.1 M phosphate buffer at pH 6.8 (Feder and O'Brien 1968).

The F.A.A. fixed materials used for plastic microtomy were dissected in the same manner as outlined for paraffin microtomy. Ovules in this state were transferred to fresh 50% ethanol, dehydrated slowly in an ethanol series, followed by three changes of absolute ethanol and two changes of propylene oxide, to ensure complete dehydration. The tissue was infiltrated with low viscosity epoxy resin (Spurr 1969) over a period of five days, then embedded in Beem capsules and polymerized overnight in a vacuum oven at 65 degrees C. The plastic blocks were sections on a Reichert OMU2

ultramicrotome with a DuPont diamond knife at 1.0 um to 1.5um then mounted on gelatin coated glass slides (Jensen 1962). The P.A.S. reaction (periodic acid-Schiffs) was utilized to stain the cell walls and starch by the localization of the total insoluble polysaccharide (Jensen 1962). The conventional cytoplasmic stains used on epoxy embedded material proved to be more troublesome with the F.A.A. fixed ovules. This is probably due to two facts: 1) there is a rather narrow range of staining procedures than can be used on epoxy sections (O'Brien unpublished) regardless of the fixative used and 2) F.A.A. is a coagulant fixative rendering the normally successful cytoplasmic stains ineffectual. To compensate, the sections were counter stained in 0.05% toluidine blue in 2.5% $Na_2 CO_3$ at pH 11.1 (Trump et al. 1961), for 2 hours and viewed under phase contrast optics.

The ovules to be fixed in 3% phosphate buffered glutaraldehyde were prepared for fixation in the field by dissecting away as much of the surrounding tissue as was possible. Ovulate cones illustrating megasporogenesis ranged in size from 2mm to 3mm. Prior to fixation the three pairs of cone bracts were removed. In the more mature cones, beyond the early free nuclear stages of the gametophyte, each ovule was dissected away from the cone and fixed. The outer integument was removed from all ovules beyond the 256 nucleate stage of gametophyte development. The tissue was then placed in vials containing 3% phosphate buffered glutaraldehyde for 24 hours at 0 degrees C. After several rinses with cold phosphate-buffer (pH 6.8), the tissue was dehydrated in a cold ethanol

series followed by three changes of absolute ethanol and three changes of propylene oxide. The tissue was embedded and sectioned as described previously for the F.A.A. fixed material. The sections were stained with P.A.S. procedure to localize the total insoluble polysaccharide component and counterstained with either aniline blue black (Fisher 1968) or 0.05% toluidine blue O in benzoate buffer at pH 4.4 (Feder and O'Brien 1968). Sudan IV was used to identify lipophilic structures; Ruthenium red was utilized to locate pectic substances (Jensen 1962; Sterling 1970).

All observations were made with a Zeiss photomicroscope II. Both brightfield and phase contrast optics were routinely used. Micrographs were taken on Kodak Plus-X film and processed in Microdol-X developer for 9 minutes at 20 degrees C.

RESULTS

Megasporangiate Cone

The megasporangiate cone (figure 1) arises as a reproductive bud in the axil of a leaf. The cone consists of a short axis bearing three pairs of decussate bracts (figure 1). Two ovules develop in the axils of the two uppermost bracts (figures 1, 5). That the two ovules are in fact axillary and not terminal on the cone axis is shown early in the ontogeny of the megasporangiate cone by the presence of a cone apical meristem between the ovules (figures 2, 4). The cone meristem (figure 4) retains the tunica-corpus type of apical organization, though the cells

are being crushed by the growing ovules. The pycnotic nuclei within the epidermal layer of the meristem suggest that the meristem has become non-functional. Normally both ovules will develop to maturity but sometimes one will prematurely abort. In such instances the initial signs of degeneration appear in the nucellus (figure 3).

The orthotropous ovule consists of a conical nucellus enclosed by two integuments which appear asymmetric in median longitudinal view (figure 5).

Megasporogenesis

A single sporogenous cell develops in the second hypodermal layer of the nucellus (figure 6). This cell, more or less ovoid in longitudinal view, is larger and histologically distinct from adjacent nucellar cells. The sporogenous cell is light staining, vacuolate and contains a translucent nucleus (figure 6). The division of the sporogenous cell into a parietal and megaspore mother cell was not observed, though an axillary file of primary parietal cells surmounting the megaspore mother cell is evident in figure 7. The number of periclinal divisions of the parietal cell appears to be variable (figures 7, 8, 9). The megaspore mother cell, located in the fifth hypodermal layer of the nucellus, is recognizable by its size, large elliptical nucleus and uniform appearing cytoplasm (figure 8). The first meiotic division is transverse and produces the two cells of the megaspore dyad (figure 9). The division is equal and the dyad cells are similar in both size and morphology. The cell walls are slightly richer in insoluble

polysaccharide than in the surrounding vegetative nucellar cells. The chalazal dyad cell undergoes a second meiotic division to produce a chalazally displaced functional megaspore surmounted by a non-functional sister megaspore (figure 10). The non-functional megaspore undergoes rapid degeneration prior to any division activity in the micropylar dyad cell (figure 10). The completion of meiosis by the chalazal dyad cell prior to that in the micropylar dyad cell illustrates a temporal polarity in favor of the dyad cell which will produce the functional megaspore. Depending on the plane of division in the micropylar dyad, either T-shaped (figures 11, 13) or linear (figures 13, 15) tetrads are produced. The resulting micropylar megaspores are non-functional and degenerate. The megagametophyte develops from one uninucleate functional megaspore; thus Ephedra nevadensis is monosporic.

Megagametogenesis

The uninucleate functional megaspore is the first cell of the megagametophyte. The megaspore undergoes an extended period of free nuclear division and cellular expansion prior to the development of cell walls. Archegonia, which will produce the female gametes and function as the site of fertilization, develop at the micropylar pole of the megagametophyte.

Functional Megaspore. The megaspore cytoplasm is rather homogeneous in appearance and devoid of vacuoles (figures 11, 14). On completion of megaspore degeneration,

the functional megaspore exhibits a protoplasmic change (figure 12). Numerous small vacuoles and protein positive granular inclusions develop in the cytoplasm. The nucleus, previously translucent, becomes dense, staining with a single large spherical nucleolus which persists through the first mitotic division (figures 12, 15, 20). As the megaspore expands a large vacuole appears at each pole of the cell; the nucleus lies between these two prominent vacuoles (figure 15).

Free Nuclear Division. A mitotic division without subsequent cytokinesis gives rise to a two nucleate gametophyte. The two nuclei are at opposite poles, separated by a large central vacuole (figure 26, 28). This central vacuole, no doubt important in regulation of gametophyte expansion and in the later parietal displacement of the free nuclei, is formed by coalescence of several small vacuoles (figures 19, 20). The micropylar nucleus divides once to produce a three nucleate gametophyte (figures 27, 30), followed by division of the chalazal nucleus to yield the 4-nucleate stage (figure 29). This indicates that the process of free-nuclear division is non-synchronous, at least during early megagametophyte ontogeny. The synchrony of mitotic divisions was not observed in older gametophytes, though the number of free-nuclei in these gametophytes were multiples of two suggesting that the nonsynchrony is ephemeral. No evidence of a micropylarly directed wave of mitotic divisions as suggested by Lehmann-Baerts (1967) was found in the gametophyte of Ephedra nevadensis. Successive

nuclear divisions occur in the parietal cytoplasm (figures 37, 39, 42), concurrent with an expansion of the central vacuole such that a gametophyte containing two hundred and fifty-six nuclei is obtained (figure 46).

Cell Wall Formation. Following the completion of the coenocytic stage of megagametophyte development, anticlinal cell walls are laid down centripetally from the megagametophyte wall (figure 51). Each nucleus within the advancing parietal cytoplasm is enclosed in an open-ended, radially aligned alveolus (figure 53). The alveolus appears five or six-sided in tangential view (figure 54). The anticlinal wall between contiguous alveoli appears at the level of the light microscope to be bipartite in nature (figure 54). A middle lamella could not be demonstrated histochemically. Intercellular spaces are formed between the common abutment of three alveoli (figure 54). Periclinal walls are layed down while the alveoli are open ended and prior to the gametophyte becoming completely cellular (figure 55). Since the actual process of cell division was not observed during this stage of gametophyte development, it could not be determined if the periclinal cell walls were the result of free wall formation or formed by cell plates during mitosis. The protoplasm of individual cells and alveoli is composed primarily of a vacuole with a thin peripheral layer of cytoplasm (figures 53, 55). The cell walls are extremely tenuous and discernible only in cells that have been subjected to fixation plasmolysis (figure 52). The radial alveoli extend centripetally at approximately the same rate and because of

the overall ovoid shape of the gametophyte, will close in the tapering chalazal portions prior to closing in the broader central and micropylar regions (figures 51, 52). Before the gametophyte becomes completely cellular, the peripheral cells at the extreme micropylar end of the gametophyte exhibit a cytological distinctiveness from surrounding gametophytic tissue (figure 58). These cells are small with numerous vacuoles and a somewhat richer cytoplasm. This indicates an early differentiation of the tissue region of the megagametophyte that will produce the archegonial initials and jacket cells.

Archegonial Formation. Two archegonia are differentiated at the micropylar pole. The archegonial initial, readily identifiable by its large size and polygonal shape, is surrounded laterally and chalazally by gametophytic cells and micropylarly by sporophytic nucellus (figures 57, 60). The large nucleus is displaced to the micropylar end of the cell, with the remainder of the protoplasm occupied by small vacuoles. An unequal transverse division cuts off a large basal central cell surmounted by a small densely protoplasmic primary neck cell (figure 61). Prior to further divisions of the primary neck cell, the central cell rapidly expands, maintaining the cellular morphology characteristic of the archegonial initial. The primary neck cell undergoes repeated periclinal and oblique divisions before anticlinal walls appear (figures 65, 66). Subsequent divisions in various planes give the neck cells an irregular appearance (figure 69).

Concurrent with the appearance of the archegonial initial, gametophytic cells surrounding the initial show signs of differentiation (figure 60). These cells constitute the incipient archegonial jacket cells which will ultimately form a histologically distinct bilayer around the central cell and neck cells (figures 65, 66). The archegonial jacket cells appear rectangular, uninucleate, and vacuolate during early ontogeny (figures 60, 61). As archegonial development proceeds, the jacket cells enclosing the large central cell become elongate, multinucleate, and cytoplasmically dense. The jacket cells micropylar to the central cell remain small and uninucleate, tending to integrate and become indistinguishable from the archegonial neck cells (figures 69, 72, 74). Nuclei of the jacket cells adjacent to the central cell have been observed to migrate into the central cell cytoplasm during the period of fertilization.

Fertilization. During central cell elongation, the central cell cytoplasm remains rather homogeneous and vacuolate with a single large nucleus at the micropylar pole (figures 65, 66, 69). Prior to division of this nucleus, a narrow, dense staining axial band of cytoplasm appears (figure 70). The central cell nucleus divides without subsequent cytokinesis into a micropylar ventral canal nucleus and centrally located egg nucleus. A dense staining mass of cytoplasm surrounds the egg nucleus prior to fertilization (figure 71). Following pollination, the pollen tube grows down through archegonial neck cells and

into the central cell (figure 74). The ventral canal nucleus is displaced laterally, but maintains its structural integrity during fertilization (figure 74). A stage in the process of syngamy was ascertained on one occasion. In that instance the male nucleus migrates to a chalazal position in the central cell, fusing with egg nucleus from beneath (figure 72). There is apparent fusion of the sperm membrane with egg nuclear membrane (figure 73), though this could not be ascertained at the light microscope level.

Nucellus

The ovule of Ephedra nevadensis is crassinucellate. The nucellus is composed of thin walled parenchyma cells extending basally into the chalaza of the ovule and intergrading laterally with the distal portions of the inner integument (figure 5). The limits of the nucellar tissue become clear during ovule degeneration (figure 3). The nucellus can be sub-divided into three morphologically distinct regions: micropylar, lateral, and chalazal; each region undergoes developmental and structural changes during particular phases of ovule ontogeny.

With sporogenous cell differentiation, the nucellus appears as an oblong protuberance (figures 5, 6) of the ovule primordium. Concurrent with the onset of megasporogenesis, the crassinucellate ovule is produced by repeated periclinal divisions of the parietal, surrounding hypodermal, and epidermal cells of the nucellus (figures 7, 8, 9). This micropylar cap is further accentuated by continued cellular

divisions (figures 12, 13, 31) until 12-15 layers of cells surmount the megagametophyte (figure 46). During archegonial formation, the axial cells of the micropylar nucellus undergo an elongation, dechromatization, and eventual degradation to form the inverted cone-shaped pollen chamber (figures 63, 64, 67). Prior to the division of the central cell nucleus, the excavation of the pollen chamber to the megagametophyte wall is complete (figure 70). Thus the pollen grains germinate on and grow into gametophytic tissue.

The megagametophyte, positioned within the nucellus at the level of insertion of the inner integument, expands laterally and chalazally at the expense of the adjacent nucellar cells (figures 13, 19, 38, 39). Some of the tissue lost to the nucellus by gametophyte expansion is replaced by cell divisions in the lateral and chalazal regions of the nucellus (figures 13, 41). The nucellus is never completely obliterated by the growing gametophyte. Later growth of the megagametophyte is bidirectional, acropetal and basal, while growth of the surrounding nucellus is acropetal. Thus the lower portion of the gametophyte, below the insertion of the inner integument, expands by the destruction of subjacent lateral and chalazal nucellus (figure 42). The acropetal expansion of the upper portion of the gametophyte is correlated with the elongation and division within the lateral nucellus above the insertion of the inner integument (figures 46, 48). This correlative growth between gametophyte and nucellus continues rapidly through the cellular and archegonial stages of ovule ontogeny such that the radial files

of gametophytic cells become stretched in a micropylar direction (figures 57, 64, 68). The bidirectional expansion of megagametophyte and the lack of mitotic activity in the micropylar portions of gametophyte, creates two histologically distinct regions within the mature megagametophyte (figure 68). From the uninucleate gametophyte to the 16-nucleate gametophyte (figure 39), the nucellar cells immediately adjacent to the expanding gametophyte exhibit no marked histological difference relative to neighboring nucellar tissue, other than general cytological and structural degradation. The nucellar cells involved in degradation during later stages of gametogenesis are histologically distinct from the surrounding nucellar tissue. The cell walls of these cells, particularly in the chalazal nucellus at the 256-nucleate and cellular stages of gametophyte development, are composed, to a large degree, of pectic substances (figures 49, 52, 58). A hypostase becomes discernible in the extreme chalazal nucellus during the 256-nucleate stage. The hypostase is cup shaped and composed of crushed empty cells with lipophilic cell walls (figures 47, 50, 68). The hypostase forms a marked structural and possible physiological boundary between the chalaza and the nucellus (figure 58).

Integuments

The nucellus and megagametophyte are enclosed by two integuments, radically different in morphology and function. The integuments arise in acropetal succession as a slight

protuberance on the dorsal side of the ovule (Fagerlind 1970). This dorsal dominance is apparent during later stages of ovule ontogeny only in transverse (figures 22, 23, 24) and median, longitudinal, sections (figures 5, 34, 37). The present study indicates that this dominance is reflected in the ventral and not dorsal side of the ovule.

Inner Integument. The inner integument, during sporogenous cell differentiation is seen as a collar encircling the base of the nucellus (figure 5). The early development of the inner integument is by repeated divisions of wedge-shaped apical initials (figures 17, 18). As the integument bilayer extends beyond the nucellar cap, the cell divions in the distal regions decrease, with a corresponding increase in cell vacuolation and elongation (figures 19, 37). Subsequent elongation of the inner integument is restricted to the more proximal portions (figures 19, 21). This proximal region of the inner integument intergrades with the lateral nucellus below the mid-point of the megagametophyte (figures 21, 43, 47). The integument-nucellar complex undergoes synchronous acropetal development such that in the mature ovule the inner integument could be incorrectly interpreted as an appendage derived from the nucellus (figure 68). The inner integument beyond the nucellar cap forms a cylindrically shaped micropylar tube (figures 22, 23, 35). The ventral dominance manifested by the inner integument during early stages of integument ontogeny, is seen during later stages of development as an oblique aperture on the dorsal side of the micropylar tube

(figures 23, 36). The inner integument is thus modified to function as an effective receptor of the microspores during pollination.

Outer Integument. The outer integument is initiated as a scarcely discernible ridge on the dorsal and dorsal-lateral side of the ovule primordium, soon forming a closed ring around the ovule (Fagerlind 1970). As is the case with the inner integument, the dorsal dominance is in fact a ventral dominance accentuated during later ovule ontogeny (figure 22). The outer integument, triangular in transverse section (figure 24), undergoes a brief period of acropetal elongation in the more distal region by anticlinal divisions of the integument epidermis, concurrent with cell division and elongation in the subsurface layers (figure 17). Subsequent elongation is primarily the result of intercalary cell divisions in the middle and proximal regions. During the coenocytic phase of megagametogenesis the distal region of the outer integument broadens due to periclinal divisions of the epidermal and sub-epidermal cells (figures 16, 34). The inner facing epidermal cells at the extreme distal end of the outer integument differentiate into thick-walled papillae (figure 44). The papillae grow inward and in effect provide a seal around the micropylar tube. The external epidermal cells of the outer integument lose their protoplasmic contents and become lignified at the initial coenocytic phase of megagametogenesis (figure 34). Sunken stomata occur sporadically along the external dorsal surface of the outer integument (figure 45).

Three unbranched vascular bundles enter the base of the ovule and supply the outer integument (figure 24). Two of the bundles traverse the ventral-lateral poles of the outer integument (figure 33). A third, smaller bundle extends through the median dorsal side of the outer integument (figure 34). Two branch traces enter the chalaza of the ovule (figure 32), ending below the hypostase in the mature ovule as short tracheids (figure 59).

DISCUSSION

The initiation of two ovule primordia in the axils of the distal decussate bracts, between a cone apical meristem, suggests a mode of development similar to the initiation of a vegetative bud in the axil of a leaf. That the ovule of Ephedra is in fact axillary has been questioned by Eames. According to Eames (1952) there is a strict homology in the male and female cones of Ephedra. He presents evidence to show that the microsporangium is terminal on a lateral appendage or megasporophyll initiated by the fertile shoot axis. Since the male and female cones are considered homologous, the ovule is seen as being terminal on a very much reduced megasporophyll and therefore appendicular in origin. The present study indicates that the ovule is in fact cauline. The ovule is seen as being a short axis, borne in the axil of a bract and bearing a terminal integumented megasporangium. The extreme apex of the fertile axis differentiates into the nucellus of the ovule. The nucellus during the very early stages of ovule ontogeny exhibits a pseudotunica-corpus type

of apical organization; the strict anticlinal divisions of the nucellar protoderm is interrupted by periodic periclinal divisions during sporogenous cell differentiation. The onset of periclinal divisions in the outermost layer of the nucellus has led to a disagreement on the origin and subsequent development of the sporogenous cell. Maheshwari (1935) and Sing and Maheshwari (1962) describe the sporogenous cell of Ephedra foliata and Ephedra gerardiana as hypodermal in origin. The sporogenous cell divides transversely into a parietal cell and a chalazally oriented megaspore mother cell. According to Fagerlind (1970), in a study of a variety of unnamed species of Ephedra, the megasporocyte arises directly from a periclinal division of a central-apical nucellus cell without the formation of a parietal cell. The classic interpretation of a hypodermal origin of the sporogenous cell was obtained in the study of angiosperm ovules (Maheshwari 1950). The nucellar epidermis in many angiosperm ovules maintains tunica-corpus mode of organization into late ovule ontogeny. In tenuinucellate ovules, the sporogenous cell often becomes the megaspore mother cell directly. In crassinucellate angiosperm ovules the sporogenous cell divides into a parietal cell and a megaspore mother cell. The parietal cell gives rise, by a series of periclinal divisions, to the nucellus cap. The ovule of Ephedr nsis can be compared with the crassinucellate type of lopment in angiosperms, except that periclin the nucellar epidermis contribute to the nucel cap. This loss of a distinctive tunica layer in the nucellus creates in many older ovules an axillary row of cells

from the epidermis to the megaspore mother cell. The megaspore mother cell thus appears as a product of an epidermal cell of the nucellus.

The first meiotic division of the megaspore mother cell is transverse producing two equal megaspore dyad cells. The chalazal dyad cell undergoes a second unequal, transverse meiotic division prior to the micropylar dyad cell dividing. Stewart and Gifford (1967) showed that in Ginkgo biloba, following meiosis I, the plastids and mitochondria present in the chalazal end of the megasporocyte, become segregated into the lower dyad cell that is destined to produce the functional megaspore. Kaplan (1969) demonstrated in Downingia that the first meiotic division of the megaspore mother cell is an unequal one, giving rise to a larger chalazal dyad cell. Kaplan states: "that in view of the importance of unequal divisions in the process of differentiation in general, this establishment of polarity during the division of the megaspore mother cell may be important in determining the survival of the chalazal megaspore." The early division of the chalazal dyad cell and the rapid degeneration of the sister megaspore is indicative of a similar process in Ephedra nevadensis. The functional megaspore is developmentally and temporally more advanced than the megaspore and dyad cell surmounting it. The micropylar dyad cell undergoes the second meiotic division in a longitudinal plane to produce a T-shaped tetrad of megaspores. The more common linear triads and tetrads of megaspores reported in other species of Ephedra (Land 1904, Berridge and Sandy 1907, Sing and Maheshwari 1962), also

occur in Ephedra nevadensis. Lehmann-Baerts (1967), studying Ephedra distachya, alone describes a tetrasporic mode of gametophyte development similar to that found in Gnetum and Welwitschia (Martens 1971).

Following degeneration of the micropylar megaspores, the chalazal functional megaspore takes on a new cytological morphology suggestive of a potential increase in metabolic activity. A number of small vacuoles and protein bodies aggregate at the micropylar pole. A large spherical nucleolus, which stains protein positive, develops in the megaspore nucleus. That the functional megaspore remains quiescent until the micropylar megaspores have completely degenerated is puzzling in light of the fact that it is differentiated so early in megasporogenesis.

The coenocytic phase of gametophyte development results from the enlargement of the functional megaspore accompanied by successive free nuclear divisions in the peripheral cytoplasm. The first two free nuclei are displaced to the poles of the megaspore by the central vacuole. The central vacuole originates by the coalescence of several small vacuoles. The late uninucleate megaspore possessed two large vacuoles prior to division of the nucleus. One must therefore hypothesize that these large vacuoles segment prior to or during the first mitotic division. According to Land (1904), Berridge and Sandy (1907), Maheshwari (1935), and Singh and Maheshwari (1962) all mitoses of the coenocyte are initially simultaneous, transforming to a chalazal directed "wave" of mitoses. Lehmann-Baerts (1967) contends that the mitotic wave travels

in an opposite direction from the chalazal to the micropylar pole. In Ephedra nevadensis the initial mitotic divisions are non-synchronous. The micropylar nucleus of the two nucleate gametophyte divides before the chalazal nucleus. No evidence of a similar mitotic polarity was observed in the later free nuclear stages of development. Lehmann-Baerts (1967) attributes the micropylarly directed mitotic wave to the influx of "organic materials" into the lower region of the gametophyte by the vascular system entering the chalaza of the ovule. I regard this origin of a physiological stimulus as improbable in Ephedra nevadensis due to the presence of a lipophilic hypostase enclosing the base of the ovule. The hypostase was observed by Berridge and Sandy (1907), Singh and Maheshwari (1962), and Lehmann-Baerts (1967) though its histochemical properties were not demonstrated. Lehmann-Baerts described the hypostase as being lignified at the cellular stage of gametophyte ontogeny. The hypostase comprises a multilayer of empty crushed cells with a lipid positive cell wall, forming a distinct boundary between the chalaza and the nucellus of the ovule. Cells on the chalaza side have thick PAS positive walls, scanty cytoplasm and are packed with starch. In contrast the adjacent cells of the nucellus are thin walled and free of starch. Lipophilic materials in the hypostase would seem to indicate a physiological barrier to a chalazal route of nutrient transport into the megagametophyte.

Gametophytic wall formation is heralded by the progressive advance of the parietal layer of cytoplasm toward

the central vacuole of the gametophyte. Anticlinal cell walls are laid down centripetally behind the cytoplasmic front, forming numerous radially aligned, open-ended, uninucleate alveoli. Each alveolus appears five to six-sided in cross-sectional view. While the alveoli are still open-ended, periclinal walls are deposited. It could not be ascertained if the periclinal walls were the result of cytokinesis and therefore associated with a spindle apparatus or free-forming. The latter method of wall formation was alluded to by Lehmann-Maerts (1967): "Before these alveoli reach the centre of the sac, their nucleus divides and afterwards the cytoplasm." Cooper (1935) describes the formation of cell walls in the embryo sac of Lilium henryi as being associated with the spindle apparatus of the last set of free-nuclear mitotic divisions. Newcomb (1972) suggested that the endosperm walls of sunflower are free-forming, meandering through the cytoplasm from the embryo sac wall. It would seem reasonable that some mechanism to regulate the direction of wall synthesis is operational in Ephedra nevadensis since the anticlinal and periclinal walls of the alveoli are relatively straight and uniformly spaced. Singh and Maheshwari (1967) describe the process of alveolation in gymnosperms as entailing spindle fibers which connect the neighbouring nuclei within the cytoplasmic front. According to Singh and Maheshwari the spindle fibers guides the centripetal deposition of the alveoli walls. Such fibers were not observed in Ephedra nevadensis.

Once the gametophyte has become cellular a disparity in the frequency of mitotic divisions between the micropylar and chalazal regions, creates two histologically distinct zones. The lower region is characterized by frequent mitotic divisions which delimit a compact zone of small, polygonal, densely cytoplasmic cells. The upper region of the gametophyte is organized into a radial network of loose knit highly vacuolate cells. Land (1904) recognized a third chalazalmost zone of large cells with dense cytoplasm and large nuclei. This region was termed the haustorial zone. The haustorial zone is not present in Ephedra nevadensis, at least up until the time of fertilization. There is a very obvious absence of starch in any of two regions of the gametophyte.

The archegonial initial which differentiates in the micropylar end of the gametophyte is morphologically similar to that found in many gymnosperms (Singh and Maheshwari 1967). The archegonial initial divides transversely into a large central cell and a much smaller neck initial. The first division of the primary neck cell is periclinal. According to Lehmann-Baerts (1967) the first division of the primary neck cell in Ephedra distachya is anticlinal. Further periclinal and oblique divisions displace the central cell deep into the gametophyte. The central cell is surrounded by a bilayer of jacket cells which are at first rectangular with the long axis perpendicular to the central cell. Since periclinal divisions do not keep pace with the elongation of the central cell, the jacket cells become much elongated.

These multinucleate, dense staining jacket cells are frequently referred to in the literature as the nutritive jacket (Foster and Gifford 1974), though their nutritive function has never been established. The migration of the jacket cell nuclei into the central cell cytoplasm and the eventual breakdown of the jacket cells following pro-embryo development (Land 1907) could indicate a nutritional relationship between jacket cell and embryo.

The central cell enlarges rapidly with a corresponding increase in vacuolation. Later in ontogeny the small vacuoles disappear, except for the extreme micropylar region, and the central cell cytoplasm becomes dense. Small globular protein positive structures, which resemble nuclei, appear in central cytoplasm. These are the proteid vacuoles described by Land (1904) in Ephedra trifurca. The proteid vacuoles which occur in many of the conifers and Ginkgo (Singh and Maheshwari 1957) were characterized by Camefort (1965), in a study on the fine structure of the egg cytoplasm of Pinus, to be more circumscribed portions of general egg cytoplasm. When the nucleus of the central cell divides, no cell wall is formed between the ventral canal nucleus and the egg nucleus. The absence of a ventral canal cell wall has been noted in all of the species of Ephedra described to date (Martens 1971). The egg nucleus migrates into the central cytoplasm, increasing greatly in size. A denser layer of cytoplasm surrounds the egg and extends as a long column of cytoplasm toward the base of the central cell. The ventral canal nucleus, which is ephemeral in many of the

conifers (Chamberlain 1935), maintains its integrity during fertilization. Kahn (1943) reported the fusion of the second male nucleus with the ventral canal nucleus, referred to by Kahn as "double fertilization." The sperm nucleus which fertilizes the egg does not take the most direct route through the central cytoplasm, but approaches the egg from beneath. During syngamy the egg nucleus appears ellipsoid and crackled. The external circumference of the egg and sperm are continuous suggesting a fusion of membranes and an absorption of sperm nucleoplasm into the egg nucleus.

The nucellus forms a major developmental component of the ovule of Ephedra. Unlike the nucellus in many angiosperms (Maheshwari 1950), the nucellus in Ephedra nevadensis is never completely absorbed by the expanding gametophyte. The cells of the nucellus continue to divide and elongate with the encroaching gametophyte. Nucellar development and gametophyte development are correlated. Up to the sixteen nucleate stage of free nuclear ontogeny the gametophyte tends to expand equally in all directions at the expense of adjacent nucellus. At the sixty-four nucleate stage of development the elongation of the gametophyte becomes bidirectional. Concurrent with the bidirectional expansion there is a corresponding change in the chalazal and lateral regions of the nucellus. The cell wall of the incipient degenerate nucellus becomes pectin positive. This unique cell wall component is maintained through the late archegonial stage and seems to concur with the onset of bidirectional gametophyte expansion. The accumulation of pectin like substances could be related

to its amorphous properties which could facilitate easier cell degeneration.

The portion of the gametophyte above insertion of the inner integument expands in an acropetal direction. A simultaneous and rapid elongation of the lateral nucellus allows the gametophyte to grow with the nucellus and not into it.

During archegonial formation a change is observed in the axial cells of the nucellar cap. There is a doubling of nuclei, an enlargement and elongation of cells, and an increase in cytoplasmic homogeneity in the nucellus. These cells soon become pycnotic and degenerate, creating a cavity which is the beginning of the pollen chamber. The breakdown of nucellar tissue continues and finally the nucellar epidermis, which lies over the cavity, degenerates. The pollen chamber appears as an inverted cone and extends to the gametophyte wall. The formation of the pollen chamber in Ephedra nevadensis is similar to that found by Land (1904) in Ephedra trifurca and by Favre-Duchartre (1956) in Ginkgo. Lehmann-Baerts (1967) reports that in Ephedra distachya the doubling of nuclei in all the micropylar cells of the nucellus except in the axial cells that ultimately form the pollen chamber. The most obvious possible function of a pollen chamber is to bring the pollen in close contact with the archegonia. It seems rather paradoxical in Ephedra, that such a deep pollen chamber is formed while a long row of archegonial neck cells displace the central cell deep into the gametophyte.

The integuments have been a subject of considerable controversy in Ephedra. Eames (1952) and Mehra (1950) consider the outer integument to be a result of the fusion of two bracteoles. Eames regards the inner integument as the only true integument, which falls in line with his theory that the ovule is borne in a megasporophyll. Three vascular bundles traverse the outer integument of Ephedra nevadensis: two run in the ventral-lateral angles of the flattened side of the ovule and a third bundle enters the dorsal median side. Thoday and Berridge (1912) investigated the vascular anatomy of the cones of Ephedra distachya. They reported eight vascular bundles entering the base of the female cone. Two traces enter each of the bracts so that four bundles are left in the axis; these four divide to produce the original number. Four more traces leave the axis to supply the next set of bracts and so on. A small bundle originates from each of the two traces which enter the distalmost bract. These two bundles fuse and develop toward but not into the dorsal side of the inner integument. The four axial bundles left in the cone axis supply the ventral-lateral poles of each ovule. Before entering the outer integument two branch traces per bundle are produced. These four small branch traces terminate at the base of the ovule. The course of ovule vasculature is similar in Ephedra nevadensis except that the dorsal fusion bundle enters into the outer integument and only one branch trace is produced per axial bundle such that only two traces are found at the base of the

hypotase. These two branch traces veer laterally towards the proximal region of the inner integument.

The present study regards the two envelopes as integuments which ultimately develop into the seed coat of the fertilized ovule. To quote Bierhorst (1971), "The term integument as it is generally applied throughout all seed plants is not one that carries with it interpretive commitment and may be applied to any complete ovular envelope."

List of abbreviations used for all micrographs:

AI = archegonium initial
Alv = alveolus
Ap = aperture
Arc = archegonium
Br = bract
CA = cone apex
CC = central cell
Ch = chalaza
CDy = chalazal dyad cell
CV = central vacuole
CW = cell wall
DM = degenerate megaspore
DNu = degenerate nucellus
EN = egg nucleus
FM = functional megaspore
G = gametophyte
GC = guard cell
Hy = hypostase
II = inner integument
JC = jacket cell
JN = jacket cell nucleus
Lat = lateral
M = sperm
Mc = micropylar
MDy = micropylar dyad cell
MMC = megaspore mother cell
Mt = micropylar tube
N = nucleus
NC = neck cell
Nu = nucellus
Nuc = nucleolus
OA = oblique aperture
OI = outer integument
Ov = ovule
P = parietal cell
Pa = papilla
Pc = procambium
PCh = pollen chamber
Pec = pectin substance
Ph = phase contrast
Pl = plastid
Pr = protoderm
PT = pollen tube
S = starch
Sp = sporogenous cell
V = vacuole
VCN = ventral canal nucleus
Xy = xylem

All sections are plastic embedded unless otherwise indicated. All micrographs are brightfield unless otherwise indicated. All sections are longitudinal unless otherwise indicated.

Fig. 1. Megasporangiate cone. Three pairs of decussate bracts (Br) are borne on short cone axis (Ax). Two ovules (Ov) arise in axils of the uppermost pair of subtending bracts. X 35.

Fig. 2. Megasporangiate cone apex. A cone apical meristem (CA) is positioned between two ovules indicating that the ovules are axillary and not terminal on the cone axis. Ph. X 205.

Fig. 3. Ovule degeneration. With the periodic abortion of one of two ovules, the nucellus and megagametophyte (G) degenerate first, followed by degeneration of the distal portions of the inner integument. The outer integument persists. X 208.

Fig. 4. Megasporangiate cone apical meristem. The cone apical meristem becomes determinate following ovule initiation. The meristem retains the tunica-corpus type of apical organization. The pycnotic nuclei in the protoderm suggests the meristem is non-functional. Ph. X 518.

Fig. 5. Ovule morphology. The ovule is made of of a nucellus (Nu), from which the gametophyte differentiates, enclosed by two integuments. X 210.

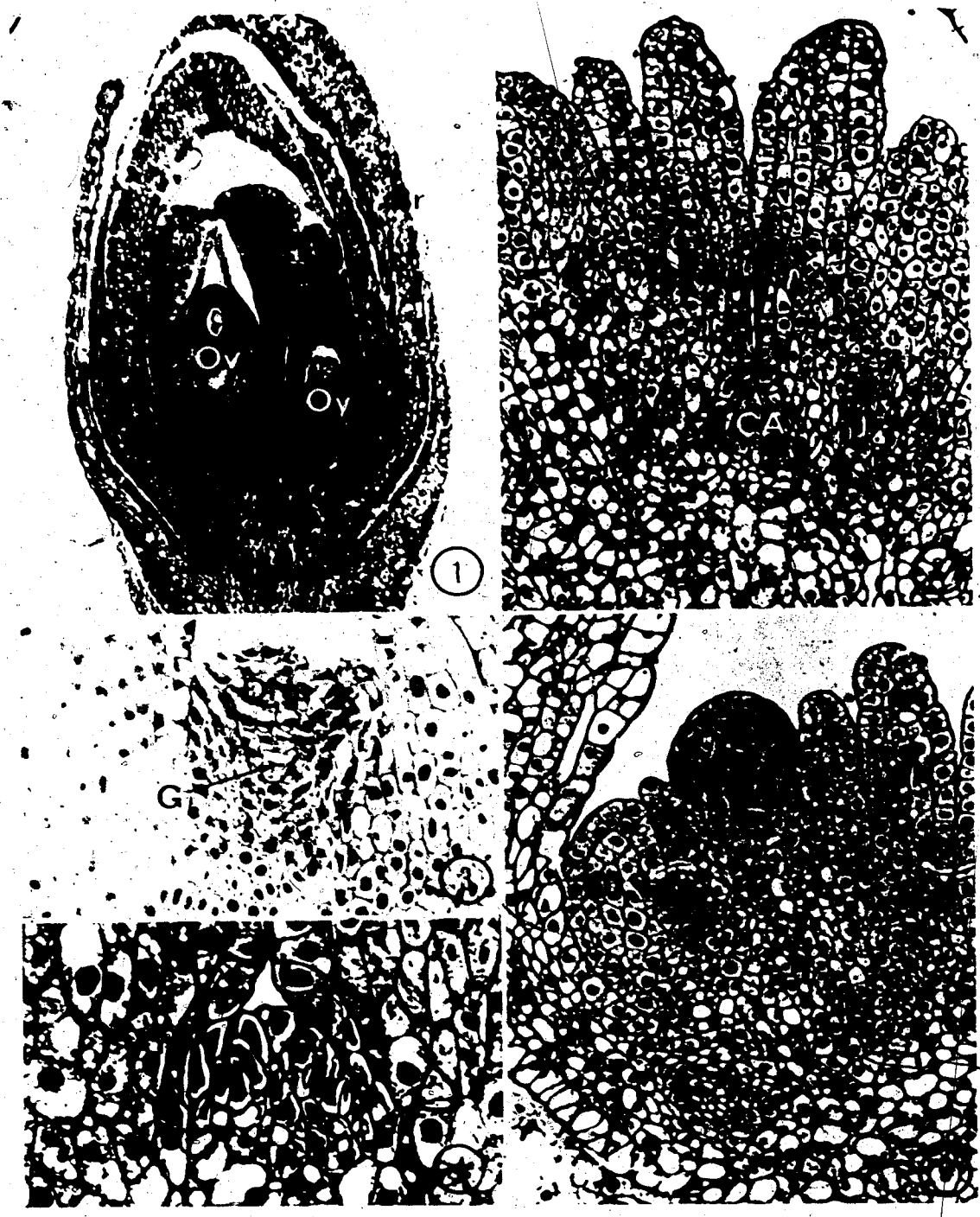
G
Ov
Ov
1
CA
G
2
3

Fig. 6. Sporogenous cell differentiation. A sporogenous cell (Sp) develops in the second hypodermal layer of the nucellus. The sporogenous cell is larger and lighter staining than surrounding nucellar cells. X 518.

Fig. 7. Periclinal divisions of parietal cell. A parietal cell (arrow) has divided twice to produce an axil row of three primary parietal cells (P). The megaspore mother cell (MMC) is partially out of the plane of section. Ph. X 510.

Fig. 8. Megaspore mother cell. A megaspore mother cell (MMC) is situated in the nucellus near the insertion of the inner integument. The primary parietal cell (P), immediately micropylar to the MMC has undergone an oblique cell division. X 518.

Fig. 9. Two cells of the megaspore dyad. Two equal axillary dyad cells are derived from the MMC following meiosis I. X 515.

Fig. 10. Chalazal dyad cell following meiosis II. The chalazal dyad cell (CDy) undergoes an apparently unequal transverse division to produce a large functional megaspore (FM) surmounted by its degenerate sister megaspore (DM). The micropylar dyad cell (MDy) has yet to divide. Ph. X 829.

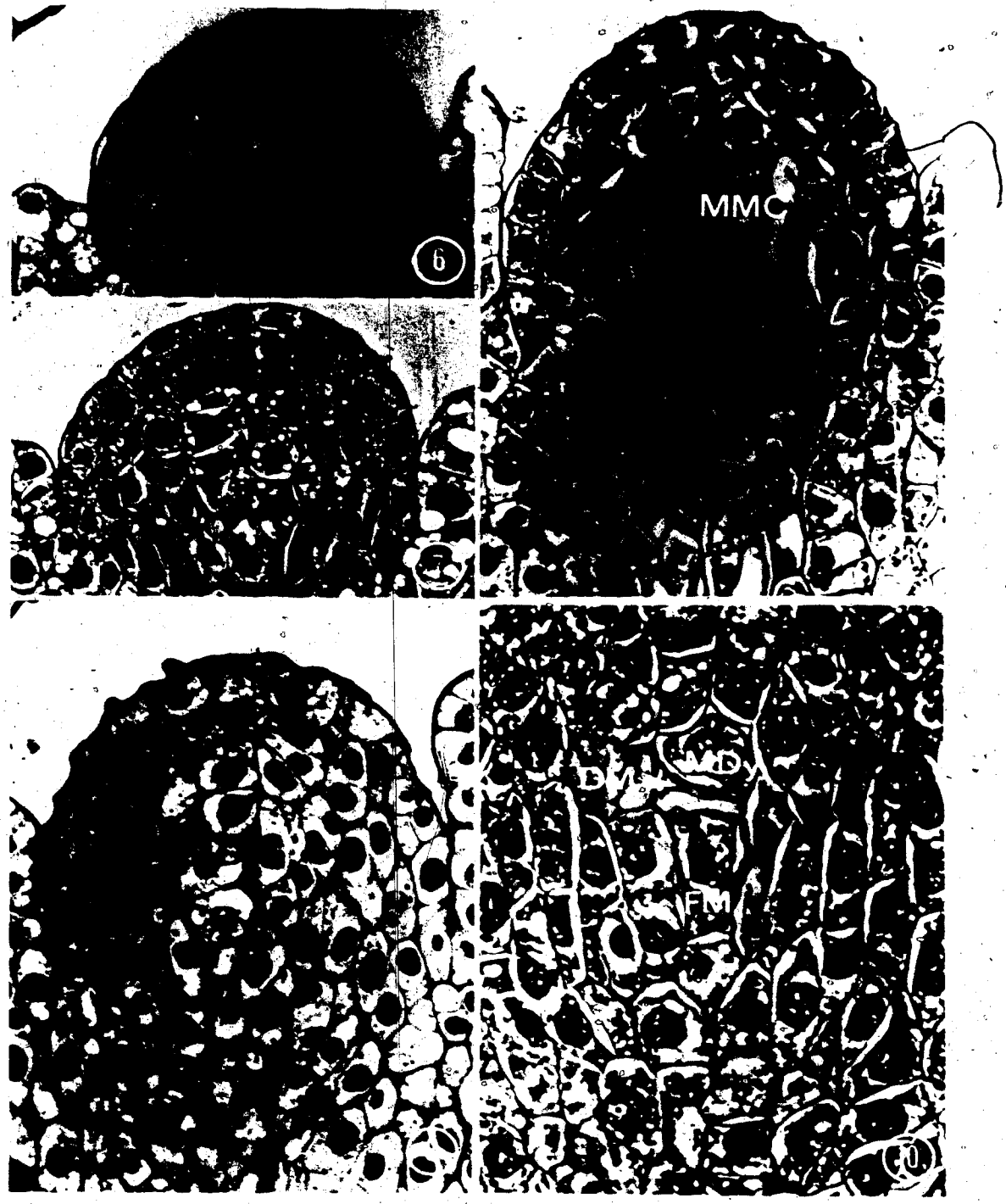
b
MMC
DM
MD
FM

Fig. 11. Tetrad of megaspores. The second meiotic division in the micropylar dyad cell is longitudinal resulting in a T-shaped tetrad of megaspores. Ph. X 518.

Fig. 12. Vacuolation of functional megaspore. Prior to expansion of the functional megaspore, numerous small vacuoles form at the lateral and micropylar poles of the cell. Numerous mitotic divisions (arrows) occur in the nucellus surrounding the functional megaspore. Ph. X 829.

Fig. 13. Expansion of the functional megaspore. Expansion of the functional megaspore is at the expense of the surrounding nucellus, primarily in the lateral portions. The nucellus is continually being replaced (arrow) by cell divisions. Ph. X 521.

Fig. 14. Tetrad of megaspores. The degenerate megaspore of the chalazal dyad cell (arrow) is obliterated by the expanding functional megaspore. Two megaspores derived from the micropylar dyad cell are in the initial stage of degeneration. Ph. X 833.

Fig. 15. Functional megaspore. Two large vacuoles (V) form at the chalazal and micropylar poles, separated by a single nucleus. A large spherical nucleolus (Nuc) characterizes the functional megaspore nucleus. Ph. X 829.

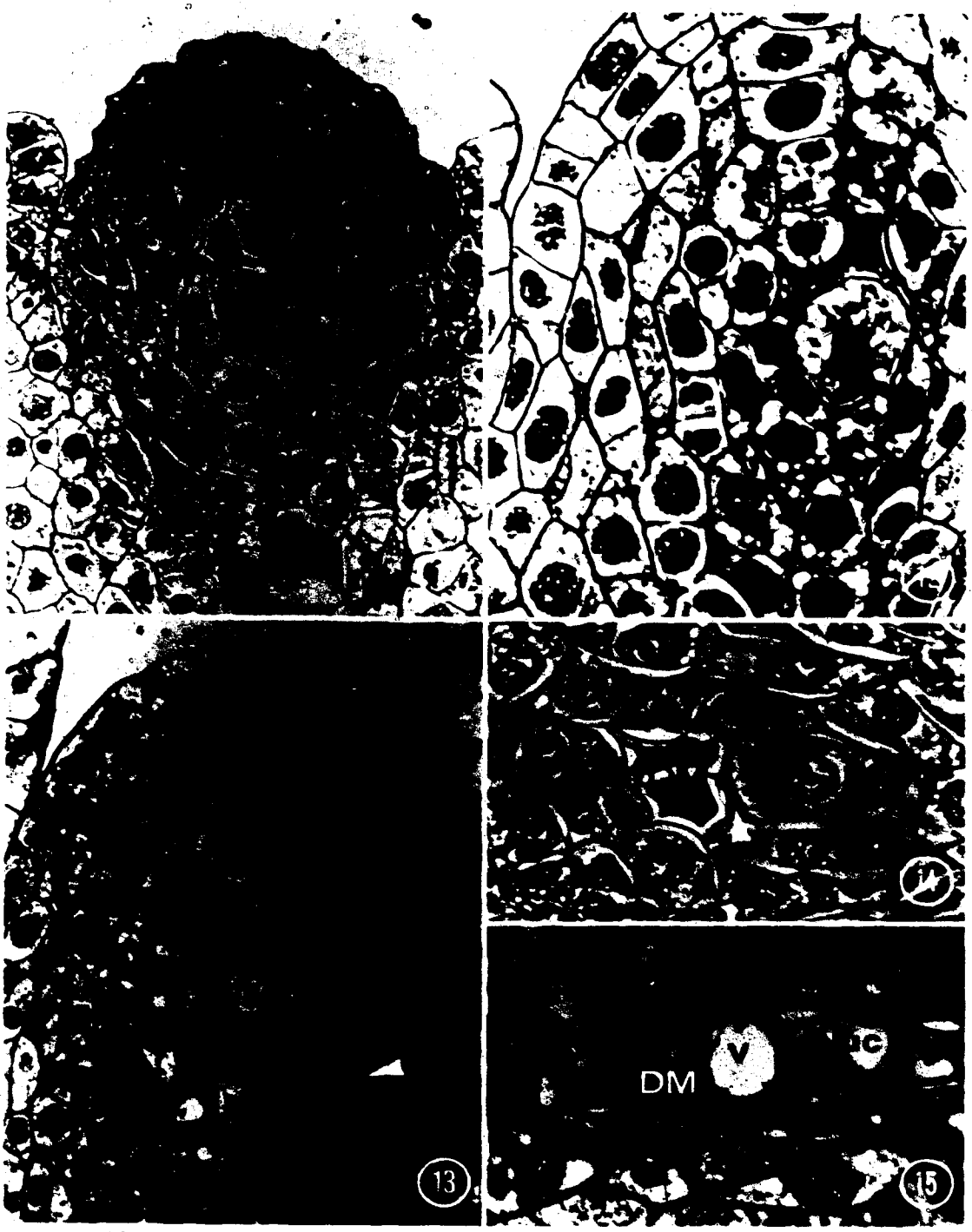
13
14
DM
V
C
15

Fig. 16. Ventral integuments at megasporogenesis. The outer and inner integuments on the ventral side of the ovule are more developed at this stage than the dorsal side of the ovule (Fig. 17). Distal portion of outer integument (OI) is beginning to expand by periclinal divisions in the sub-surface layers (arrow). X 327.

Fig. 17. Dorsal integuments at megasporogenesis. A distinctive feature of early integument ontogeny is the formation of a superficial series of wedge-shaped apical cells. Anticlinal divions maintain a protoderm in both integuments. X 324.

Fig. 18. Inner integument during functional megaspore expansion. Intercalary cell divisions (arrow) directly below the pyramidal apical initials contribute to the growth of the two-layered inner integument (II). Ph. X 331.

Fig. 19. Two-nucleate gametophyte. The inner integument bilayer beyond the nucellar cap (arrow) is characterized by large vacuolate cells. Subsequent inner integument elongation occurs in the proximal region. X 203.

Fig. 20. Two-nucleate gametophyte. The large central cell vacuole (V) is formed by the coalescence of several small vacuoles. A prominent nucleolus (Nuc) is found in each nucleus. X 329.

Fig. 21. Proximal region of the outer and inner integuments at early two-nucleate stage. Elongation of the outer and inner integuments occurs primarily in the proximal portion. The nucellus inner integument boundary (arrows) is clear. X 326.

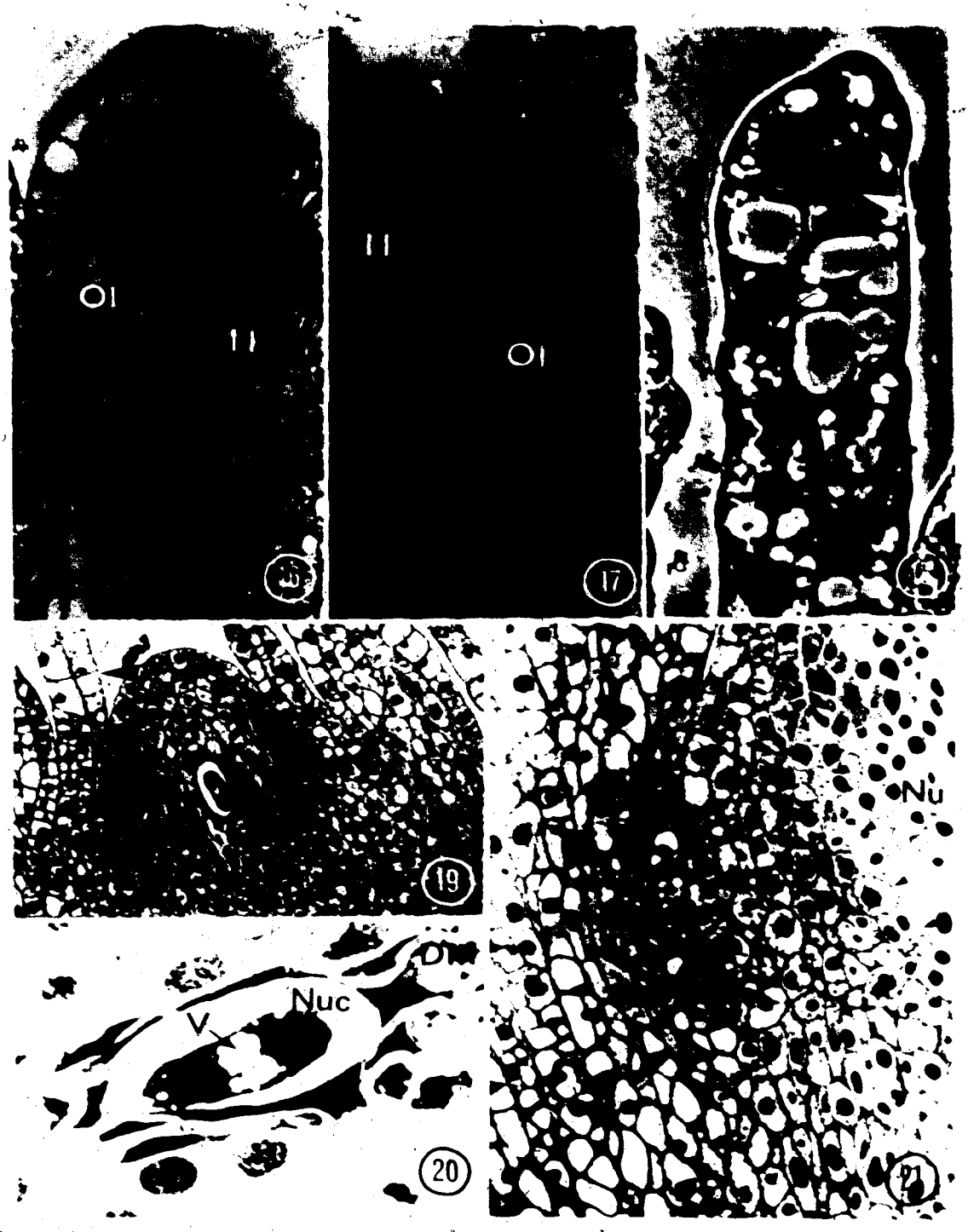
OI
II
16
II
OI
17
18
19
Nu
Nuc
V
20
21

Fig. 22. Transverse section of a young megasporangiate cone. The outer integument illustrates ventral-lateral dominance (arrows). The protoderm (Pr) of the outer integument has differentiated into thick-walled empty cells. X 129.

Fig. 23. Transverse section of a young megasporangiate cone. The outer integument is triangular with a flattened ventral side and a concave dorsal side. The inner integument is a bilayer and forms an oblique aperture (Ap) on the dorsal side. X 130.

Fig. 24. Transverse section of a young megasporangiate cone. Three unbranched vascular bundles enter the outer integument. During early gametophyte ontogeny these bundles are seen as strands of procambial cells in the ventral-lateral and dorsal poles (arrows). X 129.

Fig. 25. Two megagametophytes in a single ovule. As a rule only one megagonous cell differentiates in each ovule, although the potential for more than one gametophyte is present. Both gametophytes are two-nucleate. X 252.

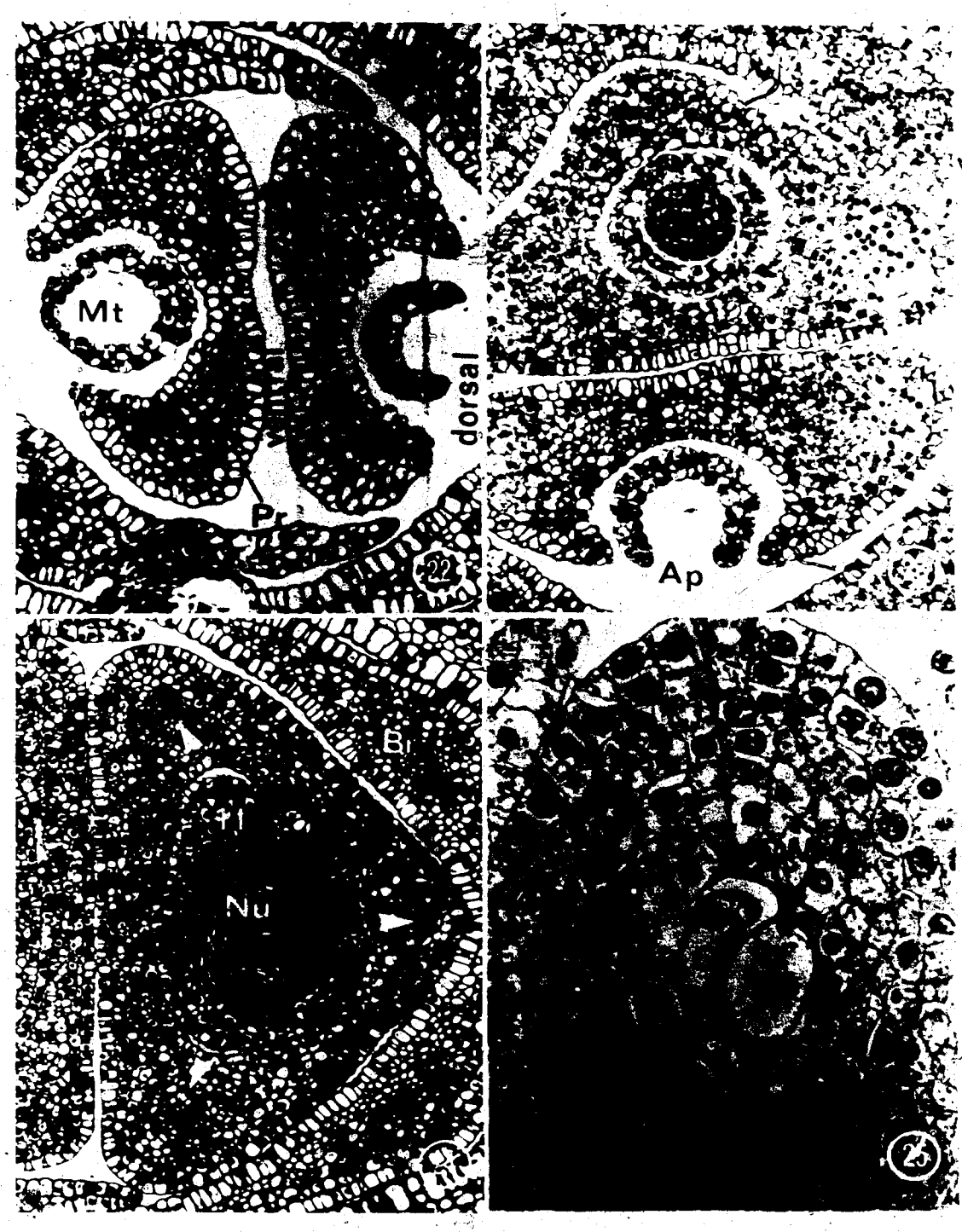
Mt
dorsal
Ap
Nu

Fig. 26. Older two-nucleate gametophyte. The central vacuole expands displacing the two free-nuclei to the chalazal and micropylar poles of the megagametophyte (G). The nucellus has expanded in a micropylar and lateral direction. Ph. X 324.

Fig. 27. Three-nucleate gametophyte. The megagametophyte continues to expand in a lateral direction. The megagametophyte maintains a position relative to insertion of the inner integument. X 206.

Fig. 28. Older two-nucleate gametophyte. Nucellar cells immediately adjacent to the megagametophyte wall have completely degenerated. A second layer of nucellus beyond the megagametophyte wall is undergoing degeneration. X 828.

Fig. 29. Four-nucleate gametophyte. The central vacuole has expanded beyond that in the two-nucleate gametophyte displacing four nuclei in a thin layer of parietal cytoplasm. Ph. X 518.

Fig. 30. Three-nucleate gametophyte. The micropylar nucleus of the two-nucleate gametophyte divides prior to the chalazal nucleus. Early free-nuclear divisions are therefore non-synchronous. Ph. X 521.

Fig. 31. Nucellar epidermis of three-nucleate gametophyte. Cells of the nucellar protoderm and of the sub-surface layers divide periclinally to produce a crassinucellate ovule. X 830.

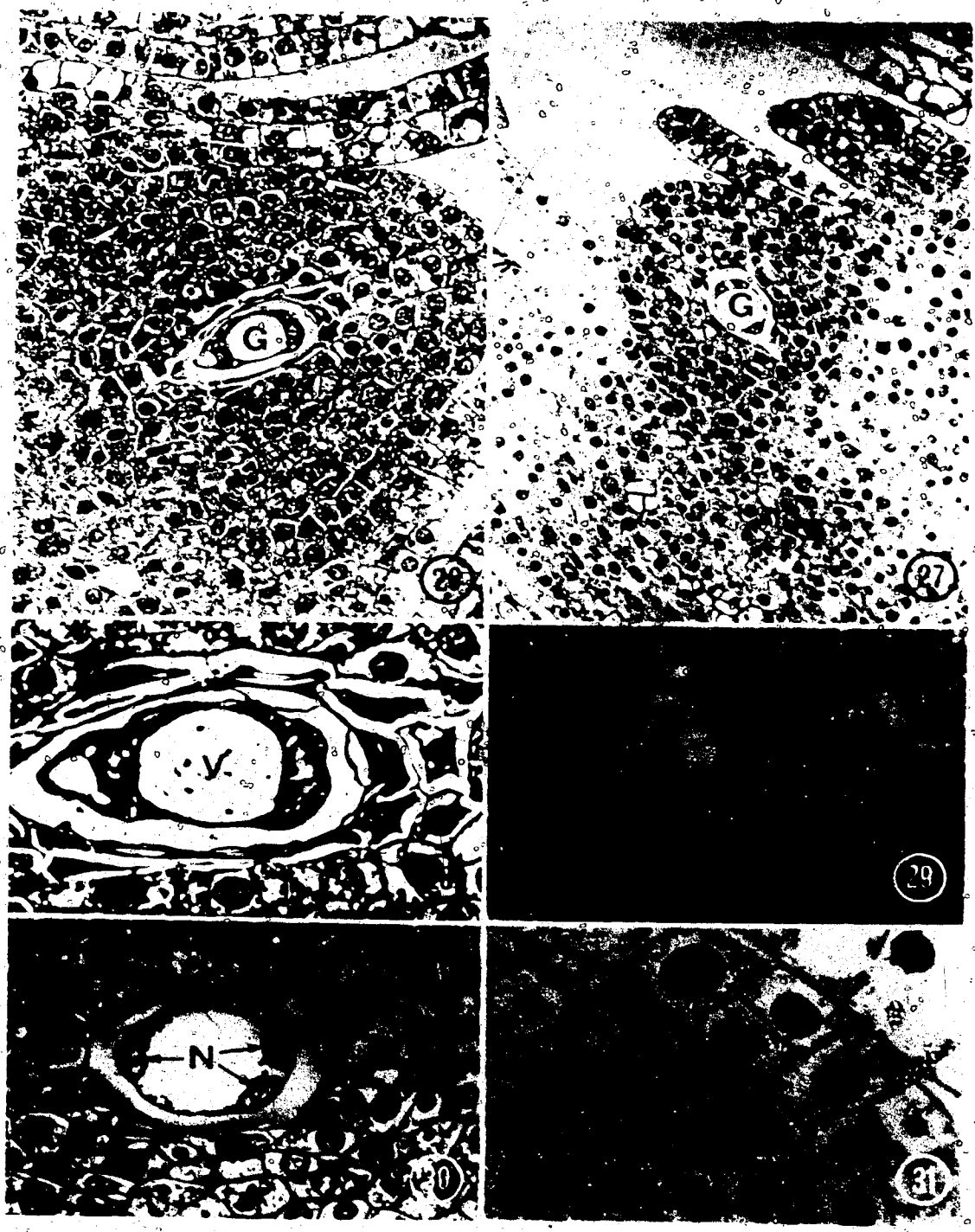
G
28
G
27
V
29
N
30
31

Fig. 32. Ovule vasculature of a two-nucleate gametophyte. Two bundles of procambial cells (Pc) enter into the base of the ovule, terminating beneath the nucellus. Each bundle develops laterally towards the inner integument but does not enter the integument. X 130.

Fig. 33. Ovule vasculature of a four nucleate gametophyte. Two procambial strands (Pc) traverse the ventral lateral poles of the outer integument (Oi) as seen in median view. X 123.

Fig. 34. Ovule vasculature of a four-nucleate gametophyte. A third strand of procambial cells (Pc) enters the dorsal pole of the outer integument. Note the formation of papillae (Pa) on the inner distal surface of the outer integument. X 130.

Fig. 35. Micropylar tube of an ovule with a sixty-four nucleate gametophyte. The micropylar tube extends beyond the nucellar cap during early gametophyte ontogeny. The long micropylar tube extends from the megasporangiate cone prior to fertilization as a result of ovular and not inner integumental elongation. X 32.

Fig. 36. Oblique aperture of micropylar tube. An extended oblique aperture develops on the dorsal side of the micropylar tube (Mt) as a result of an asymmetric development of the inner integument. X 132.

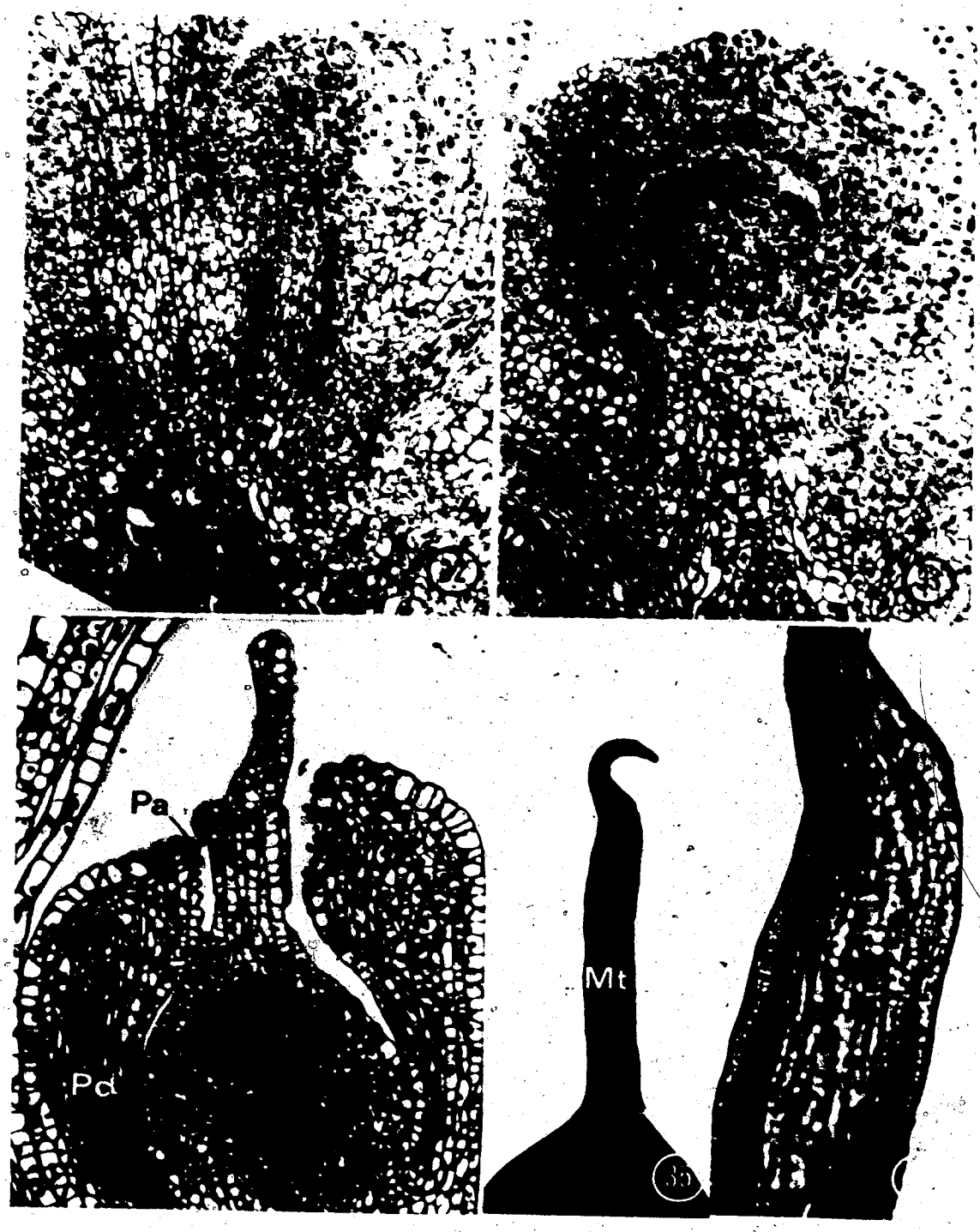
Pa
Pd
Mt

Fig. 37. Ovule with an eight-nucleate gametophyte. Cells of the inner integument beyond the nucellar cap are larger and more vacuolate than the proximal oriented cells. Distance between insertion of inner integument and outer integument has increased due to rapid development of the chalaza of the ovule. X 85.

Fig. 38. Eight-nucleate gametophyte. Tangential view of the eight-nucleate gametophyte illustrating the displacement of four nuclei in a thin parietal cytoplasm. Lateral nucellar cells are beginning to elongate, growing with the expanding gametophyte. Ph. X 324.

Fig. 39. Ovule with a sixteen-nucleate gametophyte. The inner integument has not extended beyond that seen in Fig. 37. The external protoderm of outer integument has become vacuolate and thick walled. X 129.

Fig. 40. Sixteen-nucleate gametophyte. Four nuclei (N) are seen in the parietal cytoplasm. The megagametophyte wall is rich in insoluble polysaccharides possibly derived from degenerate cells of the nucellus. Ph. X 800.

Fig. 41. Chalazal nucellus of sixteen-nucleate gametophyte. Periclinal divisions (arrow) occur in the chalazal nucellus. Nucellar cells in this region undergo a histological change prior to bidirectional gametophyte expansion. Ph. X 242.

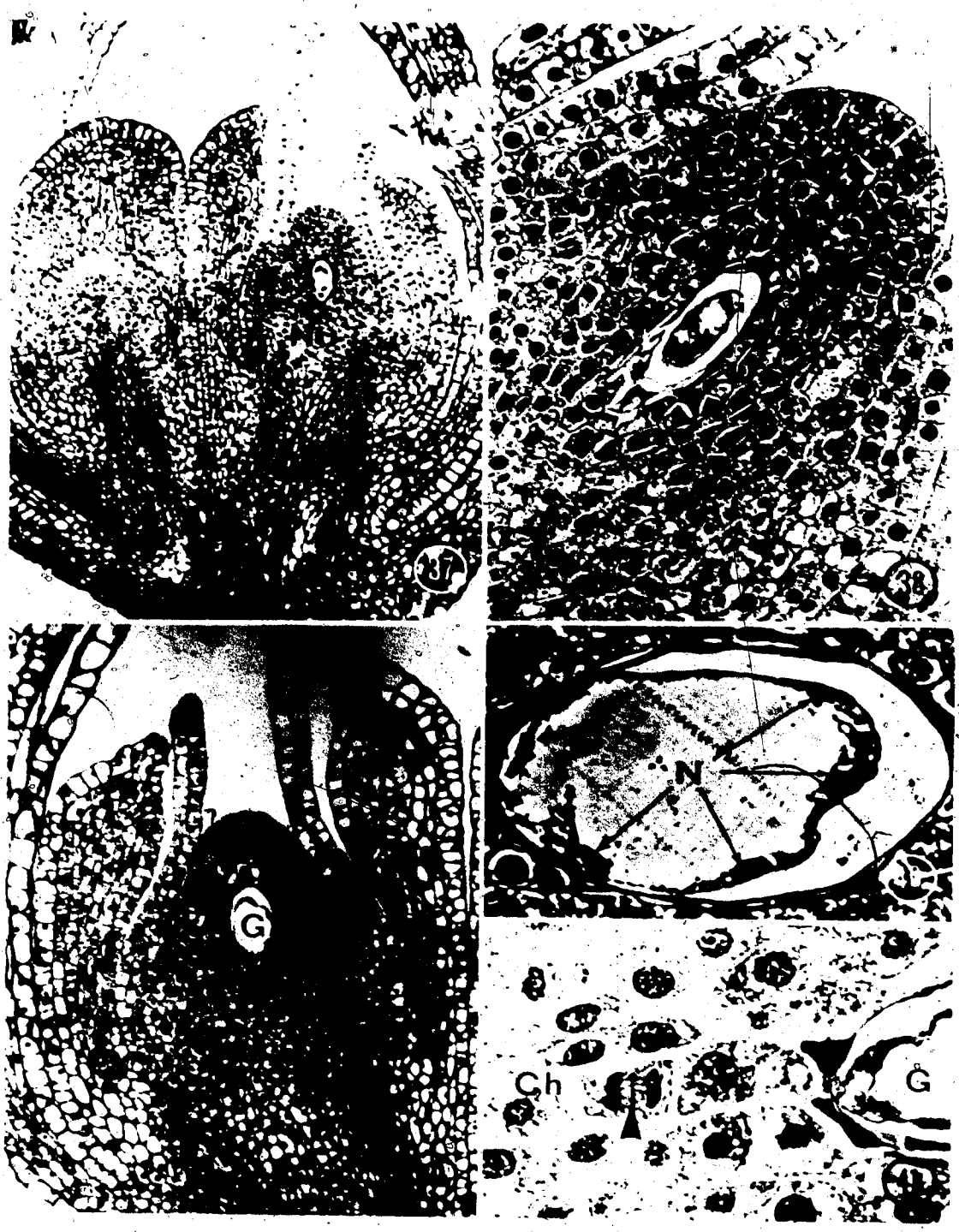
37
38
G
N
Ch
G

Fig. 42. Ovule with a sixty-four nucleate gametophyte. Cells immediately chalazal to the gametophyte (arrows) have light staining cytoplasm, indicating their impending degeneration. X 131.

Fig. 43. Chalazal nucellus of a late sixty-four-nucleate gametophyte. Cells of the chalazal nucellus below the gametophyte are beginning to degenerate. The cell walls of these cells are positive for pectic substances. The nucellus-integument boundary now appears more distinct (arrows). X 207.

Fig. 44. Distal papillae of the outer integument of a sixty-four-nucleate ovule. Papillae (Pa) develop on the inner distal surface of the outer integument forming a seal around the micropylar tube (MT). The external wall of the outer integument protoderm has thickened appreciably. X 205.

Fig. 45. Stoma in the outer integument. Stomata occur sporadically along the dorsal side of the outer integument. Numerous plastids (pl) occur in the parietal cytoplasm of the protodermal and sub-surface layers. Ph. X 518.

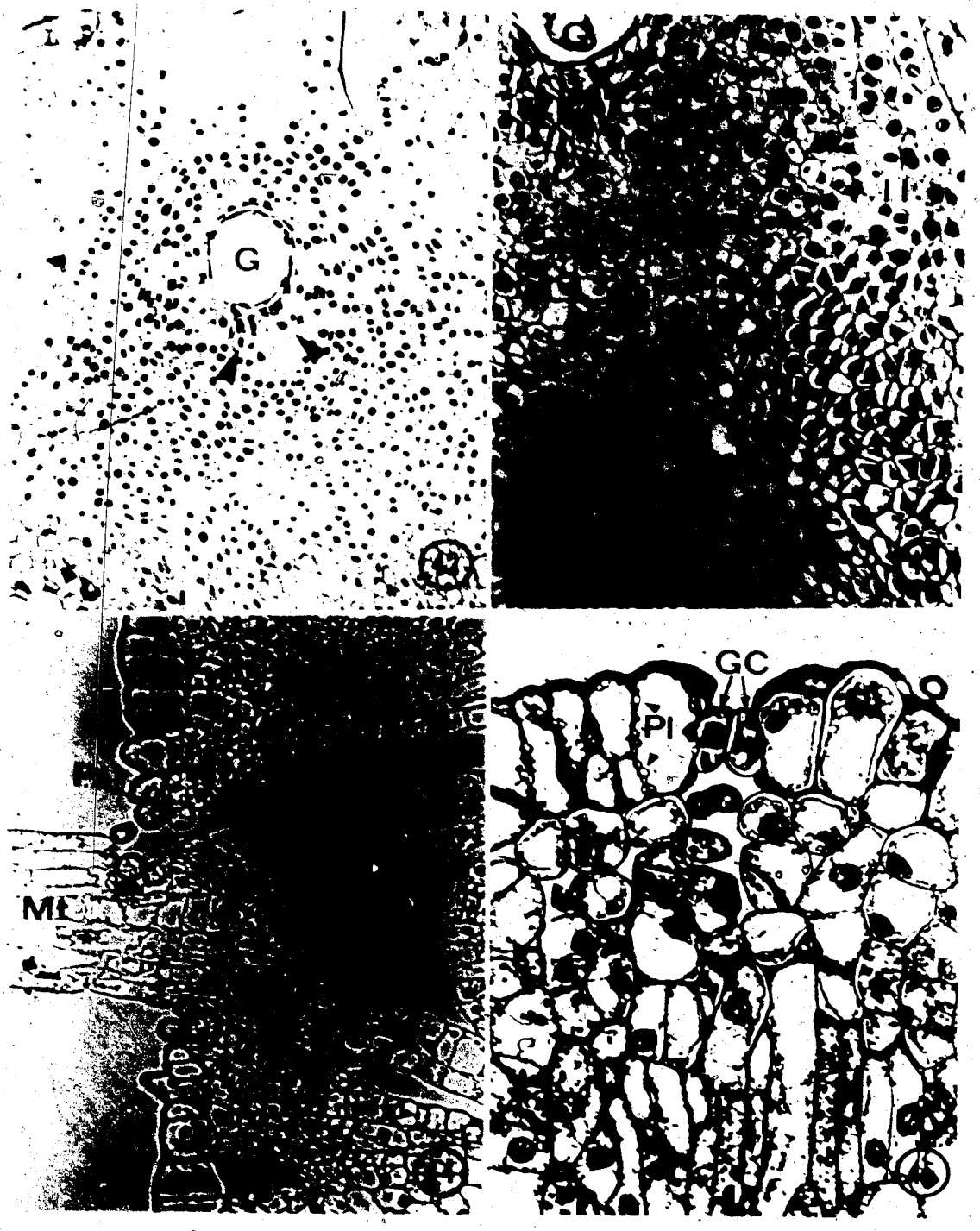
G
GC
Pl
Mt

Fig. 46. [redacted]dred-and-fifty-six-nucleate gametophyte. Elongation of the gametophyte is bidirectional, micropylar and chalazal. The mid-point of the gametophyte is at about the level of insertion of the inner integument (II). X 81.

Fig. 47. Chalaza of an ovule with two-hundred-and-fifty-six free nuclei. The chalazal end of the gametophyte expands into the chalazal nucellar cells. A lipophilic hypostase (Hy) forms an apparent physiological boundary between the chalaza of the ovule and the nucellar tissue. X 165.

Fig. 48. Lateral nucellus of an ovule with two-hundred-and-fifty-six free nuclei. The lateral nucellus between the insertion of the inner integument and the nucellar cap (arrows) elongates rapidly to compensate for the micropylar growth of the gametophyte. Repeated anticlinal divisions of the lateral nucellus protoderm occur concurrent with cell elongation in the subsurface layers. X 205.

Fig. 49. Chalazal-lateral region of a multinucleate gametophyte. The nucellus degenerates prior to encroachment of the gametophyte. The cell walls of the incipient degenerate nucellar cells are composed of primarily pectic substances. X 324.

Fig. 50. Hypostase in chalaza of the ovule. The hypostase completely encloses the chalazal nucellus. Transection. X 210.

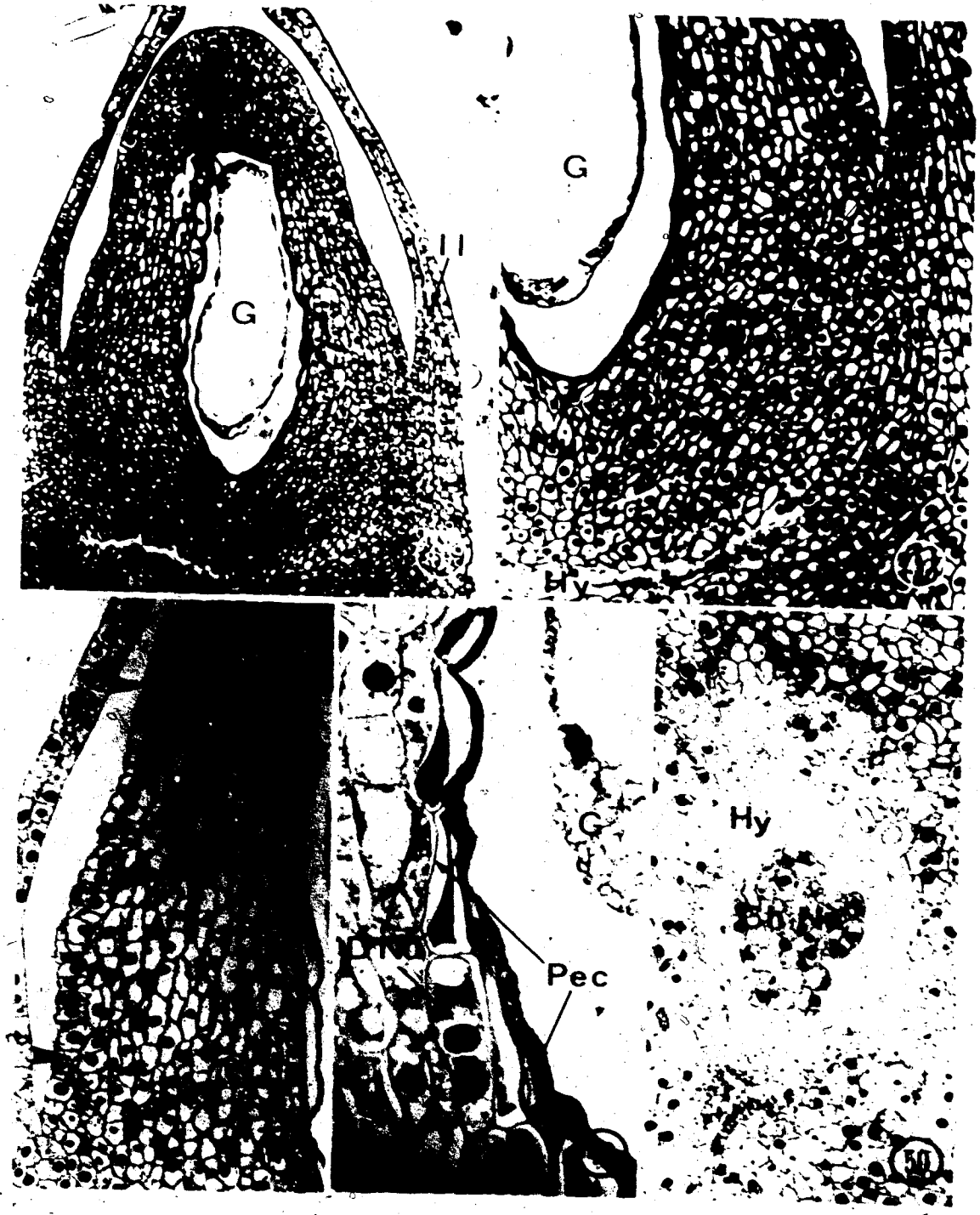
G
G
Hy
G
Hy
Pec

Fig. 51. Formation of cell walls in the gametophyte. Periclinal cell walls are deposited in a centripetal direction from the gametophyte wall. The nuclei (N) remain in the advancing cytoplasmic front. X 128.

Fig. 52. Chalazal end of the gametophyte during cell wall formation. The advancing alveoli will close in the chalazal regions of gametophyte prior to closing in the central and micropylar regions. Alveoli cell walls are tenuous and only visible in cells that have been plasmolyzed. X 512.

Fig. 53 Longitudinal section of an alveolus. The protoplasm of individual alveoli (Alv) is made up of primarily vacuole with a thin layer of parietal cytoplasm. X 320.

Fig. 54. Transverse section of an alveolus. The alveolus is five to six sided in transverse view. Intercellular spaces are formed between the common abutment of three alveoli. X 498.

Fig. 55. Periclinal cell wall formation in an alveolus. Periclinal cell walls (CW) are layed down while the alveolus is open ended. Two radially aligned nuclei (N) occupy a common cytoplasm. X 510.

Fig. 56. Micropylar end of gametophyte during cell wall formation. The micropylar gametophyte cells are small, dense staining, and vacuolate. X 510.

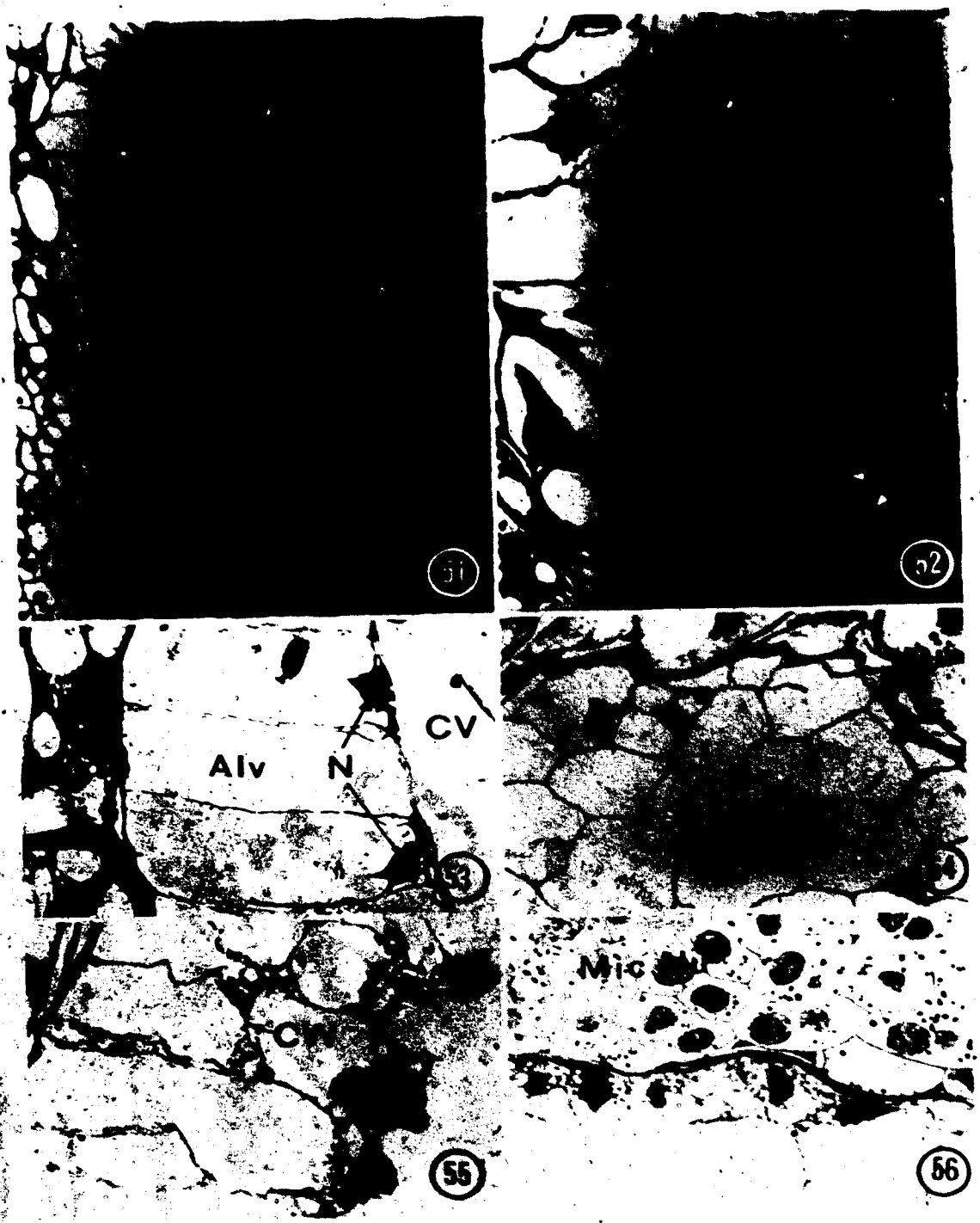
51
52
Alv
N
CV
53
Chr
55
Mic
56

Fig. 57. Archesporial initial. The archesporial initial is readily identifiable by its large size relative to the neighboring integumentary cells, and polygonal shape. Integument cell initials are beginning to differentiate from cells adjacent to the archesporial initial. X 127.

Fig. 58. Chalaza of the ovule during archesporial development in monocotyledons. The hypostase (Hy) is more defined as in Fig. 57. Chalazal cells have thick polysaccharide walls and abundant starch grains (S). The raphe bundle is characterized by thin walled cells devoid of starch grains. X 210.

Fig. 59. Vascular differentiation in the region below and lateral to the ovule. The procambial strand entering the base of the ovule (Fig. 32) differentiates into short tracheary elements. Annular and helical thickenings of secondary wall are deposited by the xylem cell. X 254.

Fig. 60 Archesporial initial. The large nucleus is displaced to the micropylar end of the cell. The remainder of the protoplasm is occupied by small vacuoles. The archesporial initial is surrounded on three sides by archesporial jacket initials. Ph. X 521.

Fig. 61. Division of the archesporial initial. An unequal periclinal division cuts off a large central cell surrounded by a small primary neck cell. Ph. X 160.


S

Fig. 62. Archegonial central cell expansion. Prior to division of the primary neck cell (PC) the central cell (CC) undergoes axial elongation. The central cell nucleus is located at the micropylar pole. Ph. X 207.

Fig. 63. Pollen chamber formation during central cell elongation. The pollen chamber (PCh) is formed by the breakdown of sub-epidermal cells of the micropylar nucellus. Ph. X 160.

Fig. 64. Ovule during archegonial maturation. Radial files of gametophyte cells are stretched in a micropylar direction by the elongating lateral nucellus. X 81.

Fig. 65. Division of the primary neck cell. The primary neck cell divides twice in a transverse to oblique plane to form a single file of four cells surmounting the central cell. X 324.

Fig. 66. Division of the archegonial neck and jacket cells. The neck cells have yet to divide in the longitudinal plane. The jacket cells adjacent to the neck cells remain uninucleate. The jacket cells adjacent to the central cell appear binucleate. Ph. X 319.

Fig. 67. Pollen chamber formation. The epidermis of the nucellus above the pollen chamber (Fig. 63) breaks down to form an inverted cone-shaped pollen chamber (PCh). Cell lysis seems to occur in the nucellar cells that have become bi and tri-nucleate. Ph. X 324.

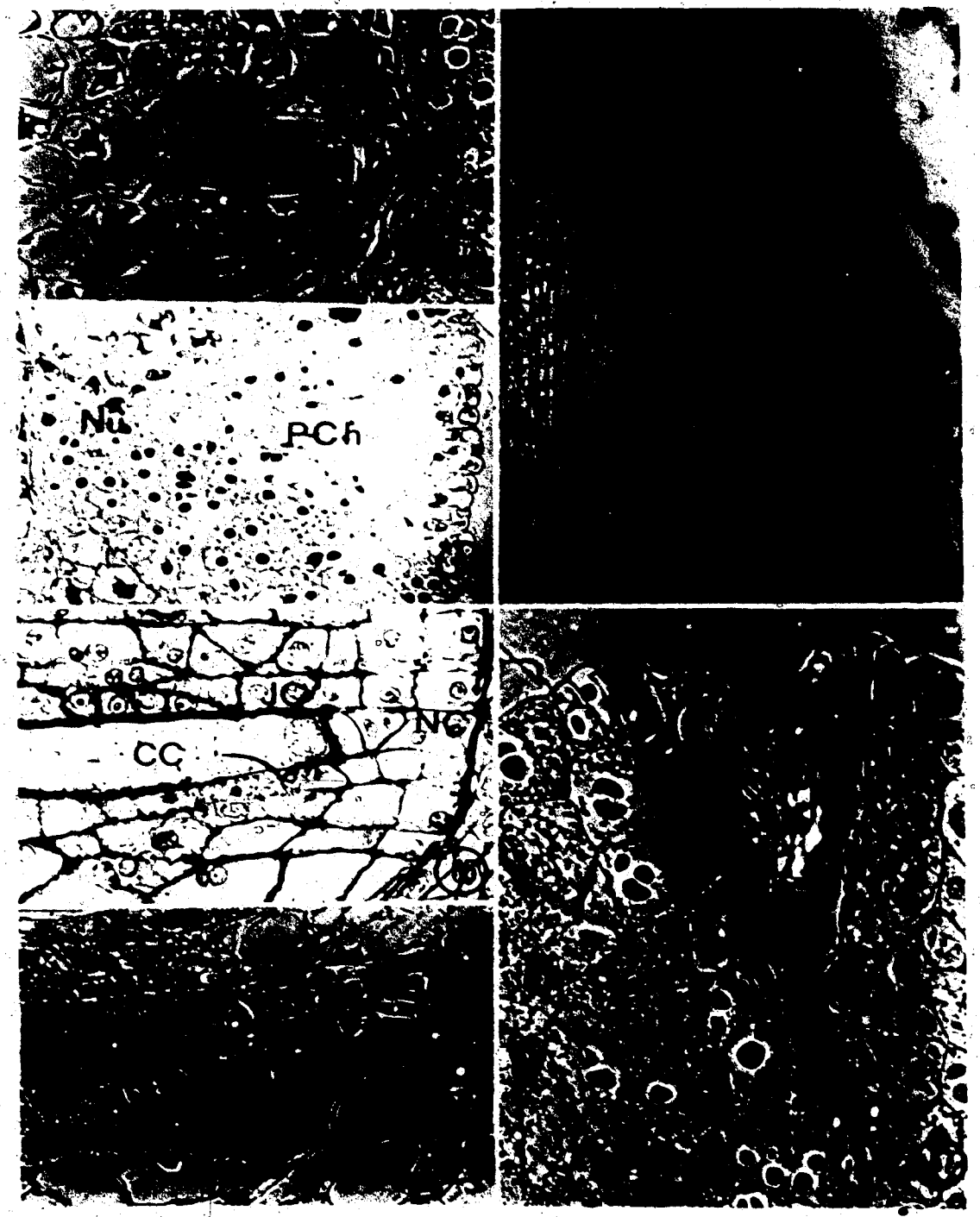
Nu
PCh
JC
NC
CC

Fig. 68. Mature ovule prior to fertilization. The mature megagametophyte maintains its previous position relative to the insertion of the inner integument. The gametophyte cells above the insertion of the inner integument are mitotically less active, lighter staining, and exhibit a stretched morphology in comparison to the small, protoplasmic chalazal gametophyte cells. Paraffin embedded. X 35.

Fig. 69. Archegonia near maturity. The central cell cytoplasm is highly vacuolate. The central cell nucleus (CCN) occupies the micropylar pole of the cell. The neck cells (NC) divide in various planes and intergrade with the micropylar jacket cells. Paraffin embedded. X 130.

Fig. 70. Ovule prior to pollination. The pollen chamber extends to the megagametophyte wall. A layer of dense staining cytoplasm surrounds the central cell nucleus. Nodules of cytoplasm (arrow) appear in the central region. Paraffin embedded. X 81.

Fig. 71. Archegonium following division of the central cell nucleus. The central cell nucleus divides mitotically without cytokinesis. The egg nucleus (EN) migrates into the mid-region of the central cell. The ventral canal nucleus maintains a position relative to the micropylar end of the central cell. The central cell cytoplasm around the egg nucleus appears dense. Paraffin embedded. X 255.


G
II
C
V

Fig. 72. Syngamy. During syngamy a layer of dense cytoplasm, prolonged in a chalazal direction, surrounds the two fusing nuclei. The male gamete fuses with egg in a position opposite and axillary to the micropylar point of entry of the pollen tube. Paraffin embedded. X 130.

Fig. 73. Syngamy. The egg nucleus is larger than in Fig. 71 and exhibits a more crackled morphology. The membranes of the sperm (S) and egg nucleus (E) would appear to be fused. The nucleoplasm of the male nucleus is continuous with the egg nucleoplasm. Paraffin embedded. X 519.

Fig. 74. Entry of pollen tube. The dense-staining pollen tube (PT) grows irregularly through the archegonial neck cells, depositing its contents into the micropylar end of the central cell. The ventral canal nucleus (VCN) is displaced laterally but does not degenerate. Paraffin embedded. X 205.

Fig. 75. Migration of jacket cell nuclei into the central cell. Immediately following the process of fertilization numerous jacket cell nuclei (JN) migrate into the central cell cytoplasm. Paraffin embedded. X 207.

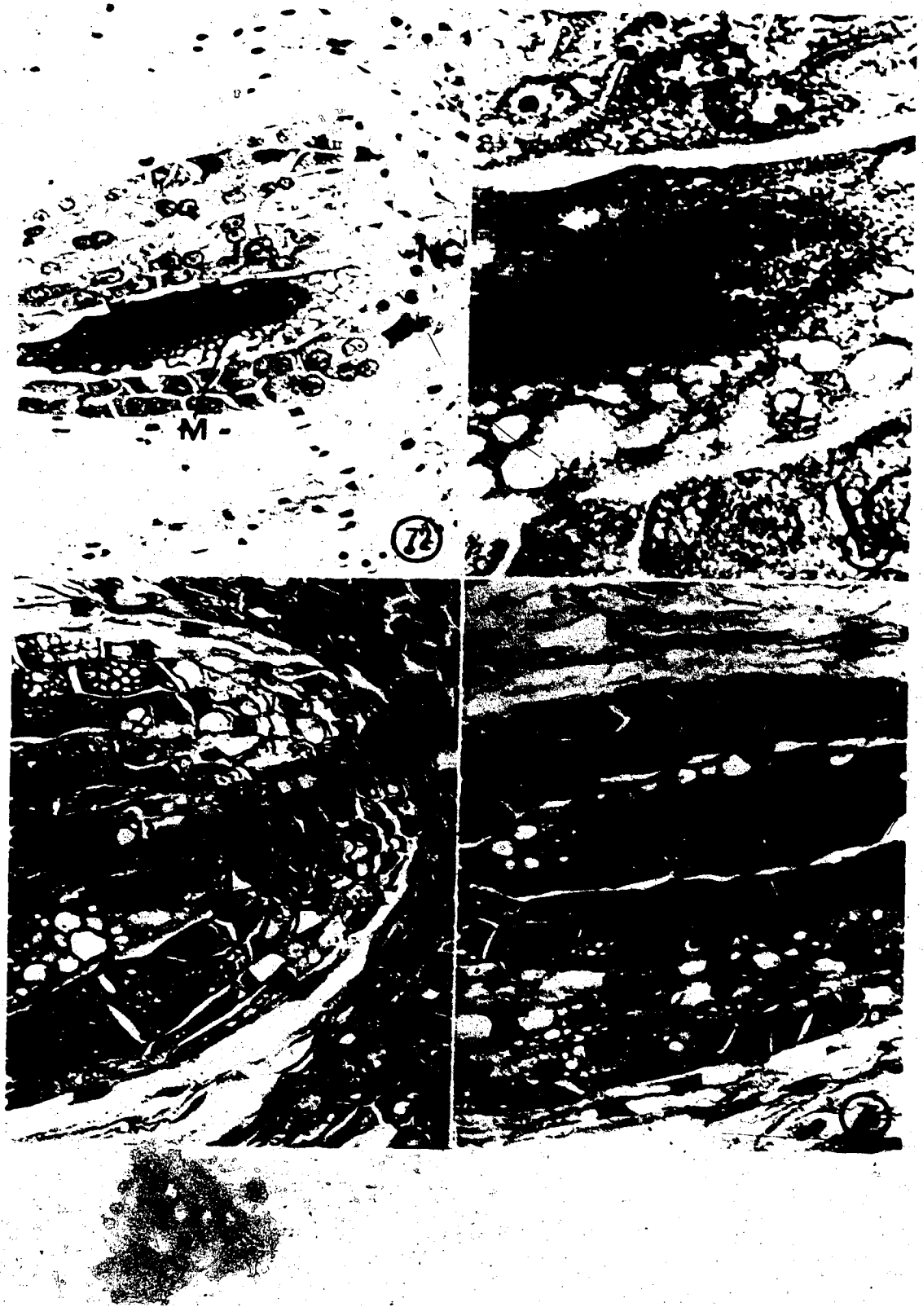
M
72

LITERATURE CITED

Andrews, H. N. 1963. Early seed plants. Sci. 142:925-931.

Arber, E. A. N. and Parkin, J. 1905. Studies on the evolution of the Angiosperms: the relation of the Angiosperms to the Gnetales. Ann. Bot. 22:489-515.

Berridge, E. M. and Sanday, E. 1907. Oogenesis and embryogeny in Ephedra distachya. New Phytol. 6:128-134.

Bierhorst, D. W. 1971. Morphology of Vascular Plants. Collier-Macmillan Canada Ltd.

Bold, H. C. 1967. Morphology of Plants. 2nd ed. Harper and Row, New York.

Brongniart, A. 1843. Enumeration des Genres de Plantes. Paris.

Camefort, H. 1965. Une interpretation nouvelle de l'organisation du protoplasme de l'oosphere des Pins. In Travaux dedies a Lucien Plantefol: 407-436. Paris.

Chamberlain, C. J. 1935. Gymnosperms. Structure and function. Univ. of Chicago Press. Chicago.

Cooper, D. C. 1935. Macrosporogenesis and development of the embryo sac of Lilium harrvi. Bot. Gaz. 97:346-355.

Cutler, H. C. 1939. Monograph of the North American species of the genus Ephedra. Ann. Missouri Bot. Gard. 26:373-428.

Eames, A. J. 1952. Relationships of the Ephedrales. Phytomorphology 2:79-100.

Esau, K. 1965. Plant anatomy. 2nd ed. John Wiley and Sons. New York.

Fagerlind, F. 1970. The initiation and primary development of the sporangia and sporangial forming organ systems in the genus Ephedra. La Cellule 68:289-344.

Favre-Duchartre, M. 1956. Contribution a l'etude de la reproduction chez le Ginkgo biloba. Rev. Cytol. Biol. Veg. 17:1-218.

Feder, N. and O'Brien, T. P. 1968. Plant microtechnique: some principles and new methods. Amer. J. Bot. 55:123-142.

Fisher, D. B. 1968. Protein staining for ribboned epon sections for light microscopy. Histochemie 16:92-96.

Foster, A. S. 1972. Venation patterns in the leaves of Ephedra. Jour. Arnold Arboretum 53:364-378.

_____ and Gifford, E. M. 1974. Comparative Morphology of Vascular Plants. 2nd ed. W. H. Freeman and Co. San Francisco.

Gifford, E. M. Jr. 1943. The structure and development of the shoot apex of Ephedra altissima Desf. Bull. Torrey Bot. Club. 70:15-25.

Jensen, W. A. 1962. Botanical Histochemistry. W. H. Freeman and Co. San Francisco.

Johansen, D. A. 1940. Plant Microtechnique. McGraw-Hill. New York.

Kahn, R. 1943. Contribution to the morphology of Ephedra foliata Boiss. II Fertilization and Embryogeny. Proc. Nat. Acad. Sci. (India) 13:357-375.

Kaplan, D. 1970. Sporogenesis and gametogenesis in Lobelia (Campanulaceae; Lobelioideae) Bull Torrey Bot. Club 97:418-434.

Land, W. J. G. 1904. Spermatogenesis and oogenesis in Ephedra trifurca. Bot. Gaz. 38:1-16.

_____. 1907. Fertilization and Embryogeny in Ephedra trifurca. Bot. Gaz. 44:273-291.

Lehmann-Raerts, M. 1967. Ovule, gametophyte femelle et embryogenese chez Ephedra distachya. Le Cellule 67:54-57.

Maheshwari, P. 1935. Contributions to the morphology of Ephedra foliata Boiss. I. The development of the male and female gametophytes. Proc. Acad. Sci. (India). 1:599-606.

_____. 1950. An introduction to the embryology of the Angiosperms. McGraw-Hill. New York.

Parkden, E. P. F. and Steeves, T. A. 1955. On the primary vascular system and the nodal anatomy of Ephedra. Jour. Arnold Arbor. 36:241-258.

Martens, P. 1971. Les Gnetophytes. (Handbuch d. Pflanzenanatomie. Band 12). Gebruder Borntraeger, Berlin.

Mehra, P. N. 1950. Occurrence of hermaphroditic flowers and the development of the female gametophyte in Ephedra foliata Boiss. Ann. Bot. 14:95-80.

Newcomb, W. P. 1972. The development of the embryo sac of sunflower, Helianthus annuus L. before and after fertilization. Ph.D. thesis, University of Saskatchewan, Saskatoon, Saskatchewan.

Parlatore, P. 1867. Flora Italiana, Vol. iv. Firenze.

Pant, D. D. and Mehra, P. 1964. Epidermal structure and development of stomata in Ephedra foliata Boiss. New Phytologist 63:91-95.

Pearson, H. W. 1929. Gnetales. Cambridge Univ. Press. London.

Singh, H. and Maheshwari, P. 1967. The female gametophyte of gymnosperms. Biol. Rev. 42:88-130.

Spurr, A. R. 1969. A low-viscosity epoxy resin embedding medium for electron microscopy. J. Ultrastruct. Res. 26:31-43.

Sterling, C. 1970. Crystal-structure of ruthenium red and stereochemistry of its pectic stain. Amer. J. Bot. 57:172-175.

Stewart, K. D. and Gifford, E. M., Jr. 1967. Ultrastructure of the developing megaspore mother cell of Ginkgo biloba. Amer. Jour. Bot. 54:375-383.

Strasburger, E. 1879. Die Angiospermen und die Gymnospermen. Jena. 1879.

Thoday (Sykes) M.G., and Berridge, E. M. 1913. The anatomy and morphology of the inflorescences and flowers of Ephedra. Ann. Bot. 26:953-985.

Thompson, W. P. 1912. The anatomy and relationships of the Gnetales. Ephedra. Ann. Bot. 26:1077-1104.

_____. 1918. Independent evolution of vessels in Gnetales and angiosperms. Bot. Gaz. 65:83-90.

Trump, B. F., Smuckler, E. A. and Benditt, E. P. 1961. A method for staining epoxy sections for light microscopy. J. Ultrastruct. Res. 5:343-348.